FACULDADE DE ENGENHARIA DA UNIVERSIDADE DO PORTO

Network Planning Model for NB-IoT

Renato Mendes da Cruz

FOR JURY EVALUATION

MASTER'S DEGREE IN ELECTRICAL AND COMPUTERS ENGINEERING

Supervisor: Prof. Manuel Alberto Pereira Ricardo

Co-Supervisor: André Filipe Pinto Coelho

September 24, 2019

Resumo

Nos últimos anos tem-se observado um crescimento acelerado no uso de tecnologias de *Internet of Things (IoT)* devido às suas inúmeras aplicações no dia-a-dia, desde *smartphones* e *tablets* até *wearables*, como *smartwatches*. Este crescimento incentivou investimentos em áreas de investigação capazes de fornecer soluções de baixo custo, procurando atingir eficiência energética e mantendo a complexidade destes dispositivos reduzida.

O elevado número de aplicações de IoT levanta desafios na gestão das redes que formam, incluindo número de dipositivos suportados, eficiência energética, cobertura e gestão dos recursos disponíveis. Para ligar estes dipositivos são utilizadas habitualmente redes *Wi-Fi*, devido à sua simplicidade de implementação e gestão, alta escalabilidade e utilização de protocolos bem definidos que garantem comunicações fiáveis, seguras e com desempenhos elevados em termos de latência e débito binário. No entanto, esta abordagem levanta alguns problemas quando se pretende uma implementação em que os dipositivos estão fisicamente distantes ou, na situação oposta, concentrados numa área reduzida. Quando se pretende projetar uma rede IoT em que os indicadores de desempenho não são regidos por latência e débito binário, mas cobertura, capacidade e eficiência energética, uma solução com redes *Wi-Fi* não é a indicada, sendo necessário explorar outras opções. Para tal, desenvolveram-se estudos focados em tecnologias de comunicações celulares de forma a perceber como é que estas seriam capazes de fornecer os serviços necessários a IoT, uma vez que este tipo de tecnologias já se encontra preparado para ligações de longo alcance e densidades elevadas de dispositivos.

Com este tipo de desafios como foco principal, esta dissertação centra-se no estudo de tecnologias existentes capazes de fornecer serviços IoT utilizando redes celulares, propondo um modelo de planeamento de redes Narrowband-Internet of Things (NB-IoT) designado NB-IoT Deterministic Link Adaptation Model (NB-DLAM) que é capaz de estimar um conjunto de métricas de Qualidade de Serviço (QoS).

Abstract

In the last years, the accelerated growth in Internet of Things (IoT) technologies, due to their numerous applications, from smartphones and tablets to wearables like smartwatches, has triggered the investment in Research & Development (R&D) areas able to develop low-cost solutions, aiming for consumption efficiency while keeping device complexity low.

The tremendous number of IoT applications gives rise to some network management issues, including the number of devices supported, power efficiency, coverage, and resources management. To interconnect these devices, Wi-Fi is usually used due to its deployment and management simplicity, high scalability, and the usage of well-defined protocols that ensure reliable, secure, and high-performance communications concerning latency and throughput. However, this approach comes with a few challenges when these requirements are not the main concern, as in networks where the devices are physically distant or, in the opposite way, in networks where there are a massive number of devices in a reduced area. To that end, studies on cellular communications were performed to understand how this type of networks would be able to provide IoT services, since they are already targeted for long-range connections and high device density.

With such challenges in mind, this dissertation focuses on the study of existing technologies able to supply IoT services over cellular networks, proposing a network planning model for Narrowband-Internet of Things (NB-IoT) named NB-IoT Deterministic Link Adaptation Model (NB-DLAM), which is able to estimate some Quality of Service (QoS) metrics.

Agradecimentos

Ao meu orientador, Prof. Dr. Manuel Ricardo, agradeço todos os seus conselhos, apoio e tempo dispendido durante o desenvolvimento desta dissertação. Ao meu co-orientador, André Coelho, toda a ajuda prestada, à sua prontidão em auxiliar no que fosse preciso, desde dúvidas teóricas até às dificuldades sentidas na parte prática do trabalho, passando pelas importantes revisões deste documento.

A chegada a este momento, a conclusão do curso, não se resume a esta dissertação. Nunca seria possível esquecer toda a caminhada até aqui chegar que começou no secundário, local onde encontrei algumas das pessoas que viriam a ser as mais importantes neste longo percurso. Aqui não poderia deixar de mencionar o João Assunção e o Tiago Sousa, que desde cedo se tornaram dois dos meus melhores amigos, companheiros do *metal* e das aulas intermináveis de *volleyball*. Naturalmente, não poderia deixar passar o Diogo Duarte e o Bruno Miranda que me marcaram unicamente neste percurso pela sua camaradagem, sei que sempre pude contar com eles para tudo, deste modo, estou-lhes eternamente agradecido. Por último, das pessoas mais importantes e que esteve sempre do meu lado, tanto para elogiar como criticar, para mandar umas gargalhadas e por sempre me aconselhar sobre tudo e sobre nada, agradeço ao Pedro Leite.

Boa disposição, amizade e muito trabalho preencheram este percurso, que culmina nesta dissertação. Estes 5 anos foram marcados por muitos, aos quais não posso deixar de agradecer, começando pelo grupo que nos ajudou a todos a ultrapassar esta fase final, é necessário agradecer todos os membros da COPA; Ao Miguel Campos, meu grande companheiro de muitas aventuras; Baltasar Aroso, por todas as palavras de encorajamento, conselhos pessoais, académicos e profissionais, as nossas conversas sobre *cybersecurity* e no fundo pela amizade que sempre demonstrou. Por tudo isto, deixo a todos um grande obrigado.

Finalmente, à minha familia, por me aturarem quando as coisas não corriam tão bem, e mesmo assim continuarem a apoiar-me incondicionalmente. Apesar de eu passar mais tempo na FEUP do que em casa, foi por uma boa causa, sem isso, não estaria tão feliz como agora estou. Em especial à minha mãe por todo o carinho, por sempre acreditar em mim, por sempre ter feito tudo o que podia para que eu chegasse a este momento e que sempre tivesse tudo o que precisava, apesar de eu nem sempre o demonstrar, deixo aqui o maior e mais sentido agradecimento de todos.

Renato Mendes da Cruz

"The scientific man does not aim at an immediate result.
He does not expect that his advanced ideas will be readily taken up.
His work is like that of the planter - for the future.
His duty is to lay the foundation for those who are to come, and point the way."

Nikola Tesla

Contents

List of Figures

List of Tables

Acronyms and Abbreviations

3GPP	3rd Generation Partnership Project
AODV	Ad-hoc On-demand Distance Vector Protocol
AWGN	Additive White Gaussian Noise
AWR	Applied Wave Research
BER	Bit Error Ratio
BLER	Block Error Rate
BS	Base Station
BW	BandWidth
CIoT	Cellular IoT
CL	Coupling Loss
CRC	Cyclic Redundancy Check
CSS	Chirp Spread Spectrum
DCI	Downlink Control Information
DL	Downlink
DRX	Discontinuous Reception
DSSS	Direct-Sequence Spread Spectrum
e-CFR	Electronic Code of Federal Regulations
EARFCN	E-UTRA Absolute Radio Frequency Channel Number
EC-GSM-IoT	Extended Capabilities-GSM-IoT
eDRX	extended-Discontinuous Reception
eNB	enhanced Node B
EPC	Evolved Packet Core
ETSI	European Telecom Standards Institute
FCC	Federal Communications Commission
FDD	Frequency Division Duplex
FFT	Fast Fourier Transform
GPRS	General Packet Radio Service
GSM	Global System for Mobile Communications
HARQ	Hybrid Automatic Repeat Request
IoT	Internet of Things
ISM	Industrial, Scientific, and Medical
LOS	Line-of-Sight
LPWAN	Low-Power Wide-Area Network
LTE	Long-Term Evolution
LTE-M	LTE for Machine-type Communication
M2M	Machine-To-Machine
MCL	Maximum Coupling Loss
MCS	Modulation-Coding Scheme

MIPS	Millions of Instructions per Second
mMTC	massive Machine Type Communications
MND	Multi-sensor Node Design
MPL	Maximum Path Loss
MT	Mobile Terminal
NB-DLAM	NB-IoT Deterministic Link Adaptation Model
NB-IoT	Narrowband-Internet of Things
NF	Noise Figure
NI	National Instruments
NPBCH	Narrowband Physical Broadcast Channel
NPDCCH	Narrowband Physical Downlink Control Channel
NPDSCH	Narrowband Physical Downlink Shared Channel
NPRACH	Narrowband Physical Random Access Channel
NPSS	Narrowband Primary Synchronization Signal
NPUSCH	Narrowband Physical Uplink Shared Channel
NR	New Radio
NRS	Narrowband Reference Signal
ns-3	Network Simulator 3
NSSS	Narrowband Secondary Synchronization Signal
OAI	OpenAirInterface
OAI-CN	OAI Core Network
OAI-RAN	OAI Radio Access Network
OFDM	Orthogonal Frequency-Division Multiplexing
OLSR	Optimized Link-State Routing Protocol
OSA	OpenAirInterface Software Alliance
PDR	Packet Delivery Rate
PER	Packet Error Ratio
PRB	Physical Resource Block
PSM	Power Saving Mode
QoS	Quality of Service
R&D	Research & Development
RAN	Radio Access Network
RE	Resource Element
RLC	Radio-Link Control
RPMA	Random Phase Multiple Access
RRC	Radio Resource Control
RTT	Round Trip Time
RU	Resource Unit
SC-FDMA	Single Carrier Frequency Division Multiple Access
SCS	SubCarrier-Spacing
SIB	System Information Block
SINR	Signal-to-Interference-plus-Noise Ratio
SND	Single-sensor Node Design
SNR	Signal-to-Noise Ratio
SoC	System on Chip
SPM	Standard Propagation Model
TAU	Tracking Area Update
TB	Transport Block

TBCC	Tail-Biting Convolutional Code
TBs	Transport Block size
UDP	User Datagram Protocol
UE	User Equipment
UL	Uplink
UNB	Ultra NarrowBand
VSS	Visual System Simulator

Chapter 1

Introduction

1.1 Context

The work presented in this dissertation focuses on Internet of Things (IoT), which has been growing exponentially in modern wireless telecommunications, with an expected growth of 25 to 50 billion connected devices by 2020 [1]. IoT is an interconnected network of objects which range from simple sensors to smartphones and tablets. Nowadays, these devices are usually connected through IEEE 802.11, however, such communications are limited in range. This paves the way to the usage of cellular technologies, including Global System for Mobile Communications (GSM) and Long-Term Evolution (LTE).

Recently, it has been estimated that between 2015 and 2021 the volume of devices connected to the Internet using cellular technologies will experience a compounded annual growth rate of about 25% [2]. Since GSM and LTE have been designed to attend service requirements defined by voice and broadband data, to cope with the growing requirements of IoT communications, 3rd Generation Partnership Project (3GPP) released three different technologies: Extended Capabilities-GSM-IoT (EC-GSM-IoT), LTE for Machine-type Communication (LTE-M), and Narrowband-Internet of Things (NB-IoT). All three are expected to provide reliable communications under extreme coverage conditions while preserving battery life and secure communications channels.

For this dissertation, NB-IoT was chosen as the study subject due to its unprecedented deployment flexibility justified by its minimum spectrum requirements. NB-IoT can operate in a spectrum as narrow as 200 kHz by refarming GSM carriers and reusing network infrastructures, which represents a major benefit for operators, while also being able to operate in the LTE spectrum [3].

1.2 Motivation and Problem

As previously stated, most IoT communications use IEEE 802.11, which means their range is limited to a few meters. As long-range communications are usually required in IoT scenarios, cellular networks are more suitable for this purpose. NB-IoT is a technology that enables this type

of communications by using either GSM or LTE carriers, dependent on the mode of operation. NB-IoT enables not only long-range communications but also a massive number of connected devices in a confined area, whereas in this scenario IEEE 802.11 would have too much interference that would render it unusable.

The main concerns when planning IoT networks are coverage (i.e., the number of devices connected per area unit), range, and battery consumption of the devices. This brings up a new set of implementation challenges, including 1) capacity able to support around 60.000 devices/km^2; 2) power efficiency enough so that batteries last 10 years/5Wh; and 3) ultra-low, complexity, and low-cost requirements.

An important use case of IoT is utility metters and wearables, which include some of the previously stated requirements. Since these devices can be located deep indoors, or even underground, this reduces coverage, due to the attenuation introduced by the buildings. Furthermore, in dense urban areas, many of these devices usually use the same cell, causing interference between them and making it hard for all of them to communicate properly.

As such, proper network planning, taking into account the number of devices, their density, and their location is vital to achieve the best performance; otherwise, we might end up with a network unable to provide the intended IoT services or even disrupting the services already implemented, by overflowing cellular resources in a cell, which would render regular cellular communications, like cell phone service, unable to operate.

1.3 Objectives

This dissertation aims at developing a model to estimate Quality of Service (QoS) metrics in NB-IoT networks, enabling proper network planning. To do so, the following sub-objectives will be pursued:

- Develop an NB-IoT theoretical model that takes into account the requirements of the slice massive Machine Type Communications (mMTC) that is included in 5G specifications;
- Evaluate and validate in simulation environment the developed model.

1.4 Contributions

The main contribution of this dissertation is a new network planning model for NB-IoT, named NB-IoT Deterministic Link Adaptation Model (NB-DLAM), which is able to estimate some QoS metrics. These estimations are based on the user's deployment conditions and enable the model to adjust the network configurations to meet the target requirements before deployment in the real world.

1.5 Document Structure

This document is composed of 5 chapters.

Chapter 1 is an introductory chapter, aimed at defining the context, motivation, objectives, and contributions of this dissertation.

Chapter 2 begins by presenting the state of the art on Cellular IoT (CIoT) technologies, that operate on licensed spectrum, with a brief comparison between them. Afterward, license-exempt Cellular IoT (CIoT) technologies are presented, followed by open-source network simulators that support CIoT communications. Thereafter, the theoretical concepts that are background to this dissertation are presented. At the end of this chapter, an evolution to the future 5G networks is studied, and a summary of related work on the subject is presented.

Chapter 3 presents a solution to the stated problem, followed by a description of the developed model, including the theoretical concepts that were used to estimate the QoS metrics, along with a scheduling algorithm to deal with multiple users.

Chapter 4 covers the experimental steps performed to validate the model presented in Chapter 3. This chapter includes the simulation setup, simulation scenarios, model results, and a comparison between theoretical and simulation results.

Chapter 5 concludes this dissertation with relevant conclusions withdrawn from the work carried out, as well as foreseeing future work to further improve the accuracy of the proposed model.

Chapter 2

State of Art

In this chapter, the state of the art for cellular Internet of Things (IoT) is discussed, by firstly comparing public technologies released by 3rd Generation Partnership Project (3GPP), and then analyzing licensed solutions. Afterward, some theoretical concepts that can be employed for proper network planning, Quality of Service (QoS) metrics, the parameters that influence them, and how to improve those metrics to achieve the strict Narrowband-Internet of Things (NB-IoT) requirements are presented. Lastly, an introduction to 5G massive Machine Type Communications (mMTC) and how NB-IoT will evolve towards it is presented.

2.1 Cellular IoT Technologies

This section presents Cellular IoT (CIoT) technologies that operate in licensed-spectrum, which corresponds to a part of the frequency space that has been licensed by national or regional authorities to a private company [3] and are regulated by 3GPP technical specifications.

2.1.1 Extended Capabilities-GSM-IoT (EC-GSM-IoT)

EC-GSM-IoT is a fully backward compatible solution that can be installed onto existing Global System for Mobile Communications (GSM) deployments, which by far represents the world's largest and most widespread cellular technology. EC-GSM-IoT has been designed to provide connectivity to IoT devices under challenging radio coverage conditions, in frequency deployments as tight as 600 kHz.

2.1.2 LTE for Machine-type Communication (LTE-M)

LTE-M is based on Long-Term Evolution (LTE), which by far is the fastest growing cellular technology. In the same way as EC-GSM-IoT and NB-IoT, LTE-M provides ubiquitous coverage and highly power-efficient operation. Using a flexible system bandwidth of 1.4 MHz or more, LTE-M is capable of serving end-users applications with more stringent requirements regarding throughput and latency than EC-GSM-IoT and NB-IoT.

2.1.3 NB-IoT

NB-IoT is a brand new radio access technology that reuses some technical components from LTE to facilitate operation within an LTE carrier. The technology also supports stand-alone operation. As the name reveals, NB-IoT operates in a narrow spectrum, starting from only 200 kHz, thus providing unprecedented deployment flexibility due to the minimal spectrum requirements. The 200 kHz spectrum is divided into channels as narrow as 3.75 kHz to support a combination of extreme coverage and high Uplink (UL) capacity requirements, considering the narrow spectrum deployment [3]. Chips that support NB-IoT exclusively (as opposed to those that also support LTE-M) are cheaper because they are simpler to create. A 200 kHz NB-IoT front-end and digitizer is much simpler than a 1.4 MHz LTE resource block.

NB-IoT physical channels, modulations, carrier spacing, and transmission rates are summarized in Table 2.1.

Table 2.1: NB-IoT physical channel specifications [4].

Layer		Technical feature	
Physical Layer	Uplink	BPSK or QPSK modulation	
		SC-FDMA	Single Carrier Subcarrier spacing: 3.75 kHz,15 kHz Transmission rates: 160 kbits/s - 200 kbits/s
			Multi Carrier Subcarrier spacing: 15 kHz Transmission rates: 160 kbits/s - 200 kbits/s
	Downlink	QPSK modulation	
		OFDMA Subcarrier spacing: 15 kHz Transmission rates: 160 kbits/s - 250 kbits/s	

NB-IoT uses a data retransmission mechanism on all channels, in both Downlink (DL) and UL, as presented in the following.

DL:

- Narrowband Physical Broadcast Channel (NPBCH).
- Narrowband Physical Downlink Control Channel (NPDCCH).
- Narrowband Physical Downlink Shared Channel (NPDSCH).

UL:

- Narrowband Physical Random Access Channel (NPRACH).
- Narrowband Physical Uplink Shared Channel (NPUSCH).

The data retransmission mechanism allows to obtain time diversity gain and lower-order modulation, to improve both demodulation performance and coverage performance[5, 6].

2.1.4 Comparison between CIoT standards

Both NB-IoT and LTE-M are optimized for lower complexity, reduced power consumption, deeper coverage, and higher device density [7]. As previously stated, NB-IoT uses data re-transmissions to improve coverage, while LTE-M relies on channel repetition; hence, the former provides wider and extreme coverage.

As depicted in Figure 2.1, NB-IoT provides a coverage radius that is 30% larger than LTE-M [8].

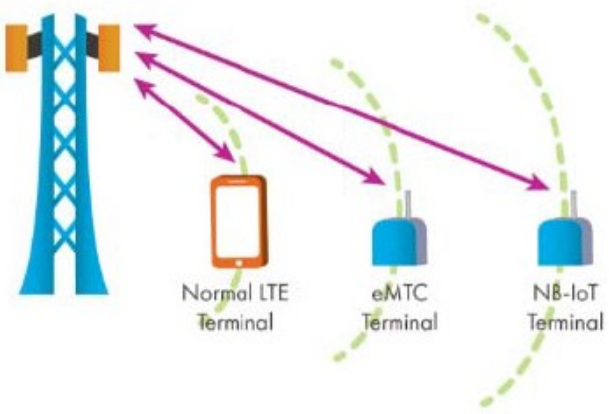

Figure 2.1: Coverage comparison between NB-IoT and LTE-M [7].

A summarized comparison between LTE-M and NB-IoT is presented in Table 2.2.

Table 2.2: Comparison between NB-IoT and LTE-M [4].

Technical index	NB-IoT	LTE-M
Coverage (Maximum Coupling Loss (MCL))	164 dB	155 dB
Power Consumption	10 years	10 years
System capacity	60.000 devices/cell	*
Voice support	No support	Limited capacity

* LTE-M does not optimize the connection count for IoT. Its predicted connection count is smaller than NB-IoT.

From the comparison presented in [7], it was concluded that NB-IoT is promising and has better performance. Compared with LTE-M, NB-IoT has a narrower band and lower peak rate, which means NB-IoT has better performance on ultra-low power consumption and low data rate services.

Although EC-GSM-IoT also expects an MCL of 164 dB, it requires an output power of 33 dB, which is 10 dB higher compared to NB-IoT. When looking in more detail, it can be concluded that NB-IoT can operate at a lower control channel Block Error Rate (BLER) than EC-GSM-IoT and LTE-M at 164dB MCL, making it more robust at extreme coverage scenarios[3].

All CIoT technologies, LTE-M, NB-IoT, and EC-GSM-IoT, can be deployed in the cellular bands just below 1 GHz and in stand-alone operation. The minimum spectrum required for such a deployment is presented in Table 2.3.

Table 2.3: Minimum spectrum requirements to deploy a CIoT network.

	Stand-Alone Deployment
EC-GSM-IoT	2×600 kHz
NB-IoT	2×200 kHz
LTE-M	FDD: 2×1.4 MHz TDD: 1×1.4 MHz

Since NB-IoT only needs a minimum of 2×200 kHz for a stand-alone Frequency Division Duplex (FDD) deployment, it can be deployed in a small part of the spectrum that remains available to the operator. For example, when an allocated band can not be fully exploited by the carrier bandwidths that are defined for LTE, then an NB-IoT carrier can be configured adjacently to the LTE carrier. The narrow system bandwidth of NB-IoT makes it suitable to also be deployed in the spectrum that is not used for mobile broadband services and remains idle. Such portions of spectrum resources can be even created by an operator, by emptying individual GSM carriers and reusing them for NB-IoT [3].

2.2 Existing Technologies

In this section, CIoT technologies that operate on license-exempt bands are discussed. For license-exempt bands, the regulations are not coordinated across regions as in the licensed spectrum [3]. These regulations change according to national regulators' rules. For example, in the United States of America, Federal Communications Commission (FCC) publishes the Electronic Code of Federal Regulations (e-CFR), which define regulations for license-exempt bands 902-928 MHz and 2400-2483.5 MHz [9], while in Europe the European Telecom Standards Institute (ETSI) regulates the 863-870 MHz [10] and 2400-2483.5 bands through the *Harmonized standards* [11].

2.2.1 LoRa Alliance

LoRa Alliance is a first example of a successful player in the Low-Power Wide-Area Network (LPWAN) market using spread spectrum technology to meet the Industrial, Scientific, and Medical (ISM) radio band regulations. LoRa uses Chirp Spread Spectrum (CSS) modulation, which is a technique using frequency modulation to spread the signal. A radio bearer is modulated with up and down chirps, where an up chirp corresponds to a pulse of finite length with increasing frequency, while a down chirp is a pulse of decreasing frequency. The LoRa Alliance claims to provide an MCL of 155 dB in the European 867-869 MHz band, and 154 dB in the US 902-928 MHz band [3].

2.2.2 Sigfox

The Signal-to-Noise Ratio (SNR) degradation calculated for a Coupling Loss (CL) of 164 dB and Noise Figure (NF) of 3dB, when BandWidth (BW) is increased from 1kHz to 1MHz, for a system operating at a transmission power of 20dBm, is proven to be linear [3]. This relationship between bandwidth and SNR is in fact used, for instance, by French LPWAN vendor Sigfox with their Ultra NarrowBand (UNB) modulation. It uses a narrow bandwidth carrier to support a claimed Maximum Path Loss (MPL) of 162 dB at 868 MHz in Europe and 902 MHz in the USA. Sigfox is among the most successful LPWAN players and supports coverage in considerable parts of Europe, including nationwide coverage in Portugal, Spain, and France [3].

2.2.3 Ingenu

A second example of an LPWAN vendor using spread spectrum is Ingenu, which uses the Random Phase Multiple Access (RPMA) technology. RPMA is a Direct-Sequence Spread Spectrum (DSSS)-based modulation complemented by a pseudo-random arrival time that helps distinguishing users multiplexed on the same radio resource. Ingenu claims to achieve an MPL of 172 dB in the USA and 168 dB in Europe. While Sigfox and LoRa Alliance are using the US 902-928 MHz band and the European 867-869 MHz band to achieve the coverage advantage associated with low-frequency bands, Ingenu is focusing on the 2.4 GHz license-exempt band [3].

2.3 Network Simulators

Several network simulators were explored and analyzed, to evaluate if they are able to simulate IoT networks, with a special focus on NB-IoT.

2.3.1 OpenAirInterface (OAI)

The OpenAirInterface Software Alliance (OSA) is a non-profit consortium fostering a community of industrial as well as research contributors for open-source software and hardware development for the Evolved Packet Core (EPC), Radio Access Network (RAN) and User Equipment (UE) of 3GPP cellular networks[1], as depicted in Figure 2.2.

The OpenAirInterface (OAI) source code is divided into two projects:

- OAI Radio Access Network (OAI-RAN).
- OAI Core Network (OAI-CN).

These projects reside in separate repositories and are distributed under separate licenses. OAI git repository has a development branch[2] for NB-IoT simulations, with full documentation of its components, API, interfaces, and design documentation[3]. Based on this branch it is possible

[1] http://www.openairinterface.org/
[2] https://gitlab.eurecom.fr/oai/openairinterface5g/tree/develop-nb-iot
[3] https://gitlab.eurecom.fr/oai/openairinterface5g/tree/develop-nb-iot/targets/DOCS/NB-IoT_Docs

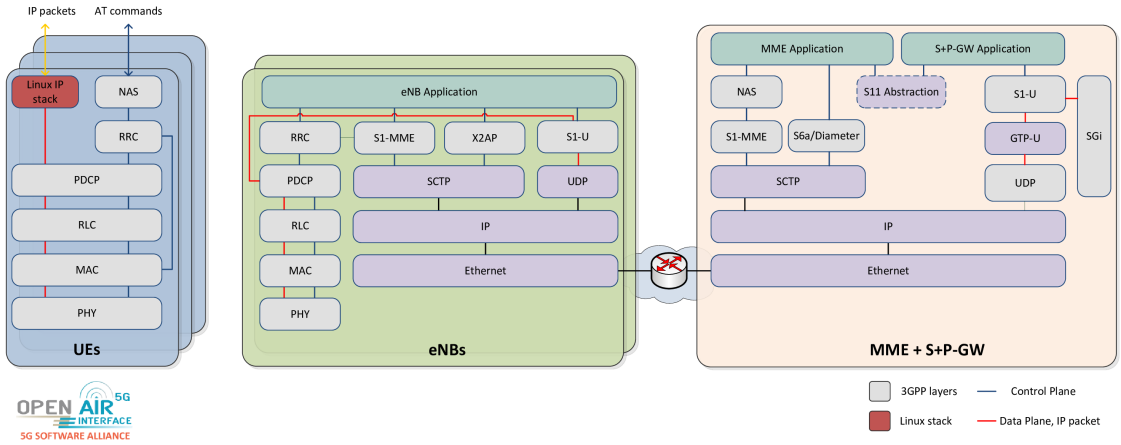

Figure 2.2: OpenAirInterface LTE software stack.

to configure: 1) the layer 2 for NB-IoT; 2) the interface between layer 2 and layer 1, which includes random access procedures, physical configurations for System Information Block (SIB), more specifically the number and periodicity of repetitions and scheduling related parameters; and 3) NB-IoT protocol stack, which includes packet structure and packet transfer for UL and DL channels[4].

2.3.2 Visual System Simulator (VSS)

Visual System Simulator (VSS) software is the system-level simulation technology that is part of the National Instruments (NI) Applied Wave Research (AWR) Design Environment platform. VSS is an RF, wireless communications, and radar systems design solution, supporting realistic measurements of cascaded RF blocks, identifying the source of spurious products, and simulating system metrics such as bit error rates[5]. Applications include:

- Circuit and System-Level Co-Simulation;
- Component Specifications;
- Communication Algorithm and Modulated Waveform Development;
- End-to-End Communications Systems (Baseband through RF and OTA);
- Wireless conformance tests for communications systems, such as:
  - 5G and LTE/LTE-A;
  - NB-IoT;
  - CDMA2000 and GSM/EDGE;
  - WLAN/802.11a/b/g and 802.11ac (IP sharing with LabVIEW).

[4]https://gitlab.eurecom.fr/oai/openairinterface5g/blob/develop-nb-iot/targets/DOCS/NB-IoT_Docs/NB_L2_interface.pdf

[5]https://www.awrcorp.com/products/ni-awr-design-environment/visual-system-simulator-software

2.3.3 MATLAB LTE Toolbox

The MATLAB LTE Toolbox provides standard-compliant functions for the design, simulation, and verification of LTE communications systems. The toolbox accelerates LTE algorithm and physical layer development, supports conformance testing, and enables test waveform generation[6]. Using this toolbox, it is possible to perform NB-IoT modeling, including:

- Create physical signals and transport channels;
- Create, encode, and decode transport channels;
- Perform Single Carrier Frequency Division Multiple Access (SC-FDMA) modulation.

With these functions, it is possible to generate DL and UL waveforms and block error rate simulation on NPDSCH and Narrowband Physical Uplink Shared Channel (NPUSCH)[7].

2.3.4 Network Simulator 3 (ns-3)

Network Simulator 3 (ns-3) is a discrete-event network simulator for Internet systems, targeted primarily for research and educational use. ns-3 is a free software, licensed under the GNU GPLv2 license, and is publicly available for research, development, and use[8]. It is supported and developed by a collection of cooperating organizations called NS-3 Consortium.

Although ns-3 core supports both IP and non-IP based networks, the large majority of its users, including this dissertation, focuses on wireless/IP simulations. These simulations involve models for Wi-Fi, WiMAX, or LTE on Layer 1 and Layer 2, although it supports a wide variety of Layer 3 routing protocols, such as Optimized Link-State Routing Protocol (OLSR) and Ad-hoc On-demand Distance Vector Protocol (AODV) for IP-based applications. Nevertheless, the main focus of this dissertation will be on Layer 1.

Although the ns-3 repository stored at gitlab[9] does not have an official branch for NB-IoT development, since 2007 an independent experimental repository[10] for NB-IoT is publicly available. However, this repository is at its early stages of development and has is stale.

In May 2019, the Research & Development (R&D) institute IMEC released a repository for NB-IoT[11]. This repository has two branches that focus on energy saving (*energy_evaluation* branch) and enhanced coverage (*repetitions_coverage* branch). The former can be used to evaluate energy consumption while the latter has major changes in the time domain to support repetitions, as well as in the frequency domain to support Multi/Single tone transmission for the UL channel [12]. To the best of our knowledge, this is the most stable implementation of NB-IoT in an open-source network simulator.

[6] https://www.mathworks.com/help/lte/gs/product-description.html
[7] https://www.mathworks.com/help/lte/nb-iot-modeling.html
[8] https://www.nsnam.org
[9] https://gitlab.com/nsnam/ns-3-dev
[10] https://github.com/TommyPec/ns-3-dev-NB-IOT
[11] https://github.com/imec-idlab/NB-IoT

2.4 Theoretical Planning

This section discusses the theoretical considerations that should be taken into account when planning a CIoT network using NB-IoT. Firstly, the communications parameters are discussed. To that end, the most used propagation models for mobile communications are described, and after that, bandwidth values for NB-IoT channels that will help to calculate the SNR are presented. After the parameters have been established, the most important QoS metrics are detailed, based on simulation results. This analysis will be of value to understand how different communications configurations affect the network performance, and how how they must be fine-tuned to achieve the strict NB-IoT requirements.

3GPP established three power classes for NB-IoT P_{tx}: 14 dBm, 20 dBm, and 23 dBm. 23 dBm is the most used in LTE.

2.4.1 Propagation Models

In wireless communication systems, data is transmitted between the transmitter and the receiver antenna by electromagnetic waves. A physical phenomenon occurs in the environment during electromagnetic wave propagation, which causes a degradation of transmitting signals, called path loss. LTE systems operating in the frequency range of 2 – 11 GHz are suitable for communications in Line-of-Sight (LOS). The path loss is characterized by two main types of models: deterministic (site-specific and theoretical-based) and empirical (statistical). Propagation prediction for LTE systems is usually conducted by empirical models [13]. Some of the most commonly used models in LTE will be studied in what follows.

2.4.1.1 Free-space Model (Log Distance)

Free space model, uses Friis equation to calculate the received power for unobstructed Line-of-Sight (LOS) paths, where power falls proportionally to $\frac{1}{d^2}$ and λ^2, as represented in Equation 2.1 [14],

$$P_{lossdB} = -K_{dB} + 10 \times \gamma \times \log_{10}\left(\frac{d}{d_0}\right) \tag{2.1}$$

where the value of K_{dB} is the free space path gain at distance $d_0 = 10 \times \lambda$, given by Equation 2.2 [14].

$$K_{dB} = 20 \times \log_{10}\left(\frac{\lambda}{4 \times \pi \times d_0}\right) \tag{2.2}$$

Common values for γ can be found in Table 2.4.

2.4.1.2 Okumura Hata Model

Okumura-Hata model is an empirical formulation of the graphical path loss data for the 150–1500 MHz band [15]. The separation distance between the transmitter and the receiver ranges from 1

Table 2.4: *Gamma* values for different environments [14].

Environment	γ
Urban macrocells	3.7 - 6.5
Urban microcells	2.7 - 3.5
Office building	1.6 - 3.5
Store	1.8 - 2.2
Factory	1.6 - 3.3
Home	3

km to 20 km, and the antenna heights may vary between 30m and 200m, and 1m and 10m, for transmitter and receiver respectively. The standard formula for median path loss in urban areas is given by Equation 2.3 [16].

$$\begin{aligned} PL_{urban}(dB) &= 69.55 + 26.16 \times \log_{10}(f_c) \\ &\quad - 13.82 \times \log_{10}(h_t) - a(h_r) \\ &\quad + (44.9 - 6.55 \times \log_{10}(h_t)) \times \log_{10}(d) \end{aligned} \tag{2.3}$$

The correction factors for mobile antenna height in a built-up environment is given by Equation 2.4 [17], for large cities, and Equation 2.5 [16] for small cities.

$$a(h_r) = \begin{cases} 8.29 \times (\log_{10}(1.54 \times h_r))^2 - 1.1, & f_c \leq 300MHz \\ 3.2 \times (\log_{10}(11.75 \times h_r))^2 - 4.97, & f_c \geq 300MHz \end{cases} \tag{2.4}$$

$$a(h_r) = [1.1 \times \log_{10}(f_c) - 0.7] \times h_r - [1.56 \times \log_{10}(f_c) - 0.8] \tag{2.5}$$

f_c - Frequency from 150 MHz to 1500 MHz (MHz)

h_t - Height of transmitter antenna (m)

h_r - Height of receiver antenna (m)

d - Distance between the receiver and the transmitter (m)

For other areas, path loss is given by Equation 2.6.

$$PL = PL_{urban}(dB) - factor_{area} \tag{2.6}$$

For Equation 2.6, the factors for suburban and rural areas can be found in Table 2.5.

2.4.1.3 Cost-231-Hata Model

It is a well-known model, applicable for the estimation of path loss in the UHF band for mobile cellular networks, which assumes that propagation between the Base Station (BS) and Mobile

Table 2.5: Okumara Hata Model loss factors for not urban areas [16].

Area	Factor
Suburban	$2 \times (\log_{10}\left(\frac{f_c}{28}\right))^2 + 5.4$
Rural	$4.78 \times (\log_{10}(f_c))^2 + 18.33 \times \log_{10}(f_c) + 40.98$

Terminal (MT) occurs in Free Space. However, it adds a term to take into account the signal behavior on rooftops and inside a street, bounded by walls on both sides [18]. The Cost-231-Hata model extends Hata's model for use in the 1500-2000 MHz frequency range, where it is known to underestimate path loss. The path loss for this model can be found in Equation 2.7 [19].

$$\begin{aligned} L_{0[dB]} &= 46.3 + 33.9 \times \log_{10}(f_c) \\ &\quad - 13.28 \times \log_{10}(h_t) - a(h_r) \\ &\quad + (44.9 - 6.55 \times \log_{10}(h_t)) \times \log_{10}(d) + C \end{aligned} \tag{2.7}$$

Where C = 0 for medium cities and suburban areas, and C = 3 for metropolitan areas. Correction factors for mobile antenna heights can be found in Equation 2.4.

2.4.1.4 Standard Propagation Model (SPM)

Standard Propagation Model (SPM) was developed based on the Hata path loss formulas [15] and is suitable for path loss predictions in the 150–1500 MHz frequency band. It determines the large-scale fading of received signal strength over a distance range of 1–20 km. Therefore, it is appropriate for the mobile channel characterization of popular cellular technologies [17]. The path loss is given by Equation 2.8.

$$\begin{aligned} P_{loss} &= K1 + K2 \times \log_{10}(d) + K3 \times \log_{10}(h_t) \\ &\quad + K4 \times DiffractionLoss + K5 \times \log_{10}(h_t) \times \log_{10}(d) \\ &\quad + K6 \times (h_r) + K7 \times \log_{10}(h_r) \\ &\quad + KClutter \times f_{clutter} + K_{hill} \end{aligned} \tag{2.8}$$

Where:

K1 - Constant offset (dB)

K2 - Multiplying factor for log(d)

K3 - Multiplying factor for log(h_t)

K4 - Multiplying factor for diffraction calculation; K4 has to be a positive number

K5 - Multiplying factor for log(d)log(h_t)

K6 - Multiplying factor for h_r

d - Distance between the receiver and the transmitter (m)

h_t - Effective height of the transmitter antenna (m)

$Diffraction Loss$ - Losses due to diffraction over an obstructed path (dB)

h_r - Mobile antenna height (m)

KClutter - Multiplying factor for $f_{clutter}$

$f_{clutter}$ - Average of weighted losses due to clutter

K_{hill} - Corrective factor for hill regions

The 'K' constants are given by Table 2.6 and the KClutter loss values for different environments are presented in Table 2.7.

Table 2.6: SPM Model constants [20].

K	Value
K1	-29.41
K2	55.51
K3	5.83
K4	0
K5	-6.55
K6	0
KClutter=1	1

Table 2.7: Clutter loss [20].

Clutter	Offset(dB)
Open	0
Inland Water	-1
Mean Individual	4
Mean Collective	6
Building	15
Village	-0.9
Industrial	12
Open Urban	0
Forest	15
Park	2
Dense Individual	5
Block Building	18
Scattered Urban	10

2.4.2 Bandwidth

In NB-IoT, the bandwidth used by each channel is well defined in 3GPP specifications, for both UL and DL, as stated in Table 2.8. These values can be used, together with the SNR, to calculate the channel capacity in terms of maximum data rate using the Shannon-Hartley theorem (c.f. Equation 3.22).

2.4.3 Quality of Service (QoS) metrics

In the following, some metrics that can be used to evaluate the QoS of an NB-IoT network are presented.

Table 2.8: NB-IoT bandwidth.

	Channel	Bandwidth (kHz)
Downlink		
	NPBCH	180
	NPDCCH	90, 180
	NPDSCH	180
Uplink		
	NPRACH	3.75
	NPUSCH	3.75, 15, 45, 90, 180

2.4.3.1 Coverage

NB-IoT defines three different coverage classes for the NPRACH channel. These classes correspond to devices with 0) Normal; 1) Extended; and 2) Extreme coverage. Normal class (0) may not need to provide NPRACH repetitions. [3].

From Figure 2.3 coupling loss is given by the loss between the transmitter and receiver after and before antenna gains, respectively. Coverage value is given by the MCL tolerated by the device, which is set to 164 dBm in NB-IoT, 20 dBm higher than General Packet Radio Service (GPRS), thus tolerating higher losses.

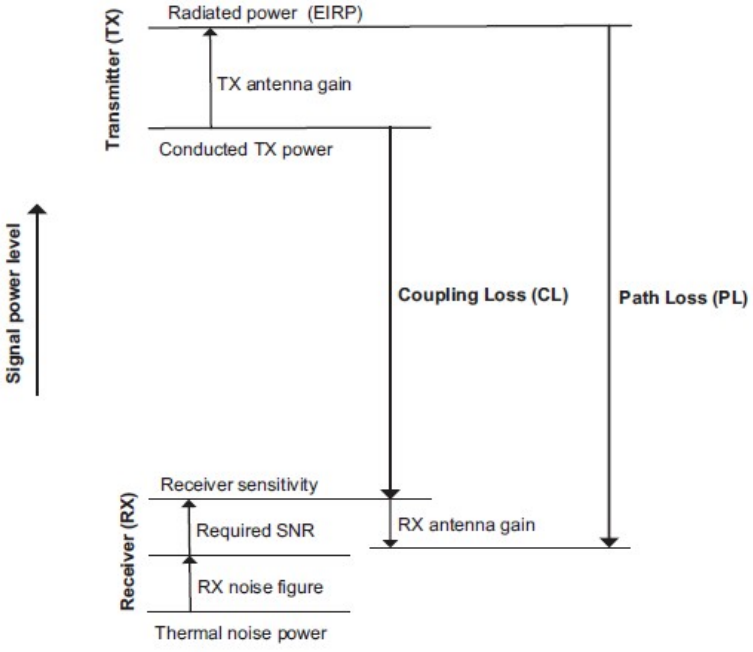

Figure 2.3: Illustration of coupling loss and path loss [3].

As stated in Subsection 2.1.3, NB-IoT uses data re-transmissions mechanisms on all channels to achieve time diversity gain and low-order modulation to improve demodulation performance and coverage performance [5, 6]. 3GPP specifies the re-transmission count for each DL (NPBCH,

NPDCCH, NPDSCH) and UL channels (NPRACH, NPUSCH) shown in Table 2.9. The number of repetitions required to correctly send a packet will affect different QoS metrics, such as latency, throughput, and battery life, and its value is influenced mainly by the device's coverage and the link's SNR.

Table 2.9: NB-IoT re-transmissions [21].

Channel		Repetitions
Downlink	NPBCH	Fixed at 64 repetitions
	NPDCCH	[1,2,4,8,32,64,128,256,512,1024,2048]
	NPDSCH	[1,2,4,8,32,64,128,192,256,384,512,768,1024,1536,2048]
Uplink	NPRACH	[1,2,4,8,32,64,128]
	NPUSCH	[1,2,4,8,32,64,128]

2.4.3.2 Throughput

For DL channels, Physical Resource Blocks (PRBs) are used to map physical channels and signals onto Resource Elements (REs), which are the smallest physical channel unit, uniquely identifiable by its subcarrier and symbol indexes within a PRB. Each PRB is composed of 12 subcarriers over 7 Orthogonal Frequency-Division Multiplexing (OFDM) symbols. Each Transport Block (TB) is mapped into one subframe, and each subframe is comprised of two slots of 0.5ms, for 15kHz of carrier spacing, and 2ms for 3.75kHz of carrier spacing, as seen in Figure 2.4. As such, each slot is composed of one PRB (c.f. Figure 2.5). This resource allocation can be used to calculate throughput, taking into account the modulation used in each subcarrier, the number of subcarriers that are used in each OFDM symbol, the number of symbols that are used per PRB, and lastly, how long a PRB lasts.

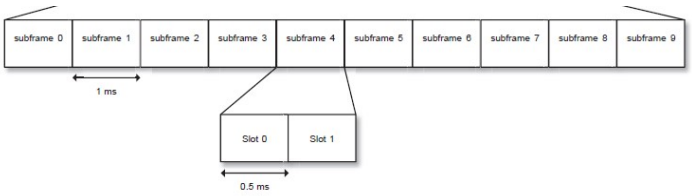

Figure 2.4: Subframe structure [3].

For UL, Resource Units (RUs) are used to map channels to REs, depending on the configured subcarrier spacing and the number of subcarriers (tones) allocated to UL transmission [3]. This configuration will impact the performance of the transmission, as fewer tones are used for harsher coverage conditions. For the most basic case, which considers 12 subcarriers with 15kHz spacing, each RU corresponds to 1 PRB.

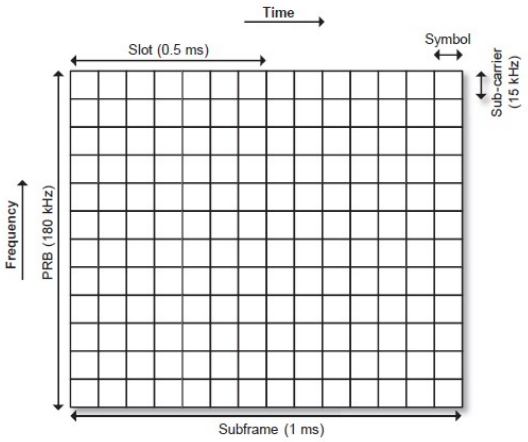

Figure 2.5: Physical Resource Block (PRB) [3].

2.4.3.3 Latency

NB-IoT metrics are mainly aimed at improving coverage, battery life, and system capacity, so latency is relaxed, although a delay budget of 10 seconds is the target for exception reports. With an MCL target of 164 dB, if a reliable transmission is provided, latency increases due to the data re-transmission mechanism.

From simulation data in [1], latency for irregular reporting service scenarios can be seen in Table 2.10 and Table 2.11, which includes latency values, for random access procedures (T_{PRACH}), resource allocation delay ($T_{allocation}$), data transmission (T_{data}) and acknowledgement delay (T_{ACK}), for different coupling losses, reliability of 99% and no data compression, for both UL and DL procedures.

Table 2.10: NB-IoT UL latency (100 bytes load) [4].

Time [ms]	Coupling loss [dB]		
	144	154	164
T_{PRACH}	142	142	142
$T_{allocation}$	908	921	976
T_{data}	142	549	2755
T_{ACK}	933	393	632

Table 2.11: NB-IoT DL latency (100 bytes load) [4].

Time [ms]	Coupling loss [dB]		
	144	154	164
$T_{allocation}$	908	921	976
T_{data}	152	549	2755

Simulations were done for both in-band and guard-band deployment. UL and DL latencies are composed of resource allocation and data transmission, while the UL also has synchronization, broadcast information reading, and random access. For the synchronization and system reading information latencies, results can be found in Table 2.12.

Table 2.12: NB-IoT synchronization latency [4].

Time [ms]	Coupling loss [dB]		
	144	154	164
T_{sync}	500	500	1125
T_{PSI}	550	550	550

From Table 2.12, the total latency taken to send and receive a packet of 100 bytes can be calculated. Results are presented in Table 2.13

Table 2.13: NB-IoT total latency.

Time [ms]	Coupling loss [dB]		
	144	154	164
T_{total}	4236	4525	9911

The time taken for a device to be served depends on the system load since when an enhanced Node B (eNB) receives more traffic from the User Equipments (UEs) it will form a queue. The offered traffic can be predicted with different traffic models, which depend on different parameters, including 1) arrival pattern of requests, 2) service pattern, 3) the number of parallel queues, 4) maximum capacity of requests in the system, and 5) order in which the requests are processed.

All these parameters will influence the system load on each eNB and consequently the total latency of the communications.

2.4.3.4 Battery Life

Battery life is mainly influenced by the device's behavior, and its Radio Resource Control (RRC) connected state duration, rather than the network. This has been studied in [22]. Assuming that DL packet arrival follows an exponential distribution with rate λ, battery consumption was modeled using the 1) sum of average consumption rates for a subframe to receive a data packet and the probability of packet arrival for the DL Hybrid Automatic Repeat Request (HARQ) Round Trip Time (RTT), 2) the NPDCCH period, 3) the extended-Discontinuous Reception (eDRX) cycle, and 4) the default paging cycle. The study concluded that it is more favorable to decrease the duration of the RRC connection state. The negative effect on battery consumption, due to unnecessary monitoring of control channels, is higher than the efficiency improvement of the data reception, as the duration of the RRC connection state increases. As the data arrival rate decreases, the duration of the RRC connection state should decrease to improve battery consumption efficiency [22].

3GPP specifies that NB-IoT devices last 10 years / 5Wh with an MCL of 164 dB. According to simulated data [1], using both Power Saving Mode (PSM) and eDRX, the results for battery life-time for different CLs, communications period and length of packets used, can be seen in Table 2.14.

Table 2.14: NB-IoT battery life estimation [4].

	Battery life [years]		
Message size / Message interval	144 dB	154 dB	164 dB
50 bytes / 2h	22.4	11.0	2.5
200 bytes / 2h	18.2	5.9	1.5
50 / 1 day	36.0	31.6	17.5
200 bytes / 1 day	34.9	26.2	12.8

After the DL HARQ RTT timer expires, the device enters in a Discontinuous Reception (DRX) inactivity time during which it periodically monitors NPDCCH for paging messages. If there are no data packets for the UE until the inactivity timer expires, it changes its state from RRC connected to RRC idle state, by receiving a connection release message [22]. After the RRC idle state expires, the device enters PSM.

In PSM, which was introduced in Release 12, the terminal is still registered online, but in deep sleep, so it is unreachable because it does not monitor the paging channel NPDCCH to receive information regarding NPDSCH messages, achieving power saving [3, 4]. Reachability in PSM is determined by Tracking Area Update (TAU), which determines the PSM cycles. For UL procedures, the device may perform random access only when it has a packet to transmit or the TAU timer expires [22].

In Release 13, 3GPP added eDRX, which further increases the sleep cycle during RRC idle state. After each eDRX cycle, a paging transmission window starts during which DL paging is possible [3].

A simplified depiction of a device's power saving cycle is represented in Figure 2.6.

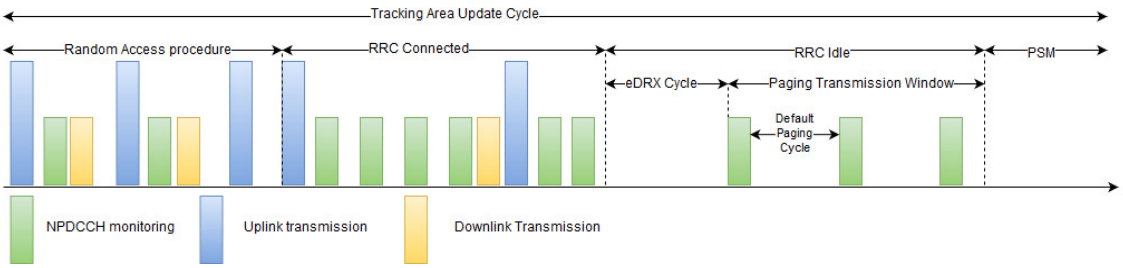

Figure 2.6: Device power saving cycles.

2.4.3.5 System Capacity

3GPP's Release 13 [8] established that NB-IoT should be capable of serving 60.000 devices, however, this value has been updated in Release 14 [23] to 6.000.000 devices [24]. NB-IoT's system capacity is achieved by using 36 narrowband channels, with 23 dBm transmitting power, reduced air interface signaling cost, improved spectrum efficiency, and simplified protocol stack [4].

NB-IoT system can be contained in GSM carriers of 200 kHz bandwidth, and to increase capacity, multiple carriers can be deployed (i.e., multiple cells or systems). However, in this narrow bandwidth, the continuous broadcast of system information and synchronization signals will take a significant part of the DL resources. Therefore, the multi-carrier operation was introduced in which there is one anchor carrier carrying this always-on broadcast signaling and possible non-anchor carriers for offloading of data traffic and increase capacity [24].

To improve capacity analysis theory of NB-IoT, researchers study the maximum number of connections supported by NPRACH and the optimal proportion of allocated resources for arbitrary random access, total constrained bandwidth, and mutual restriction among NPRACH, NPDCCH, NPDSCH, and NPUSCH [4].

Capacity evaluation of NB-IoT in an in-band deployment is presented in the technical report by Nokia Networks [25] with 12 subcarriers at 15kHz subcarrier spacing in both UL and DL. It is shown that the capacity of an in-band deployed NB-IoT system is 71k devices/cell with an information packet size of 32 bytes [26]. The capacity is defined by [1] as the rate of reports per hour: reports/h/cell. For the case of 52k devices, this number is 6.8 reports/s/cell [25].

2.4.3.6 Device Complexity

NB-IoT aims at offering competitive module prices. Like EC-GSM-IoT, an NB-IoT module can be implemented as a System on Chip (SoC). Table 2.15 presents a summary of the design parameters affecting the device complexity, for both Release 13 Category N1 and Release 14 Category N2.

The number of soft channel bits in Release 13 assumes that a maximum NPDSCH TBs of 680 bits is used, which are attached with 24 cyclic redundancy check bits and then encoded by the LTE rate-$\frac{1}{3}$ TBCC, giving rise to a maximum 2112 coded bits

Regarding baseband complexity, the most noteworthy operations are the Fast Fourier Transform (FFT) and decoding operations during the connected mode, and the Narrowband Primary Synchronization Signal (NPSS) detection, required during cell selection and re-selection procedures.

Complexity can be measured in terms of computer speed and power. Millions of Instructions per Second (MIPS) measure roughly the number of machine instructions that a computer can execute in one second. Regarding cell selection or re-selection procedures, the complexity is mainly due to NPSS detection, which requires that the device calculates a correlation value per sampling time interval. NPSS detection complexity is less than 30 MOPS [27]. Note also that the device does not need to simultaneously detect NPSS and perform other baseband tasks[3].

Table 2.15: Overview of NB-IoT device complexity [3].

Parameter	Value
Operation mode	FDD
Duplex modes	Half duplex
Rx antennas	1
Power class	20, 23 dBm
Highest order DL/UL modulation	QPSK
Maximum DL Transport Block size (TBs)	Cat N1: 680 bits Cat N2: 2536 bits
Number of HARQ processes	Cat N1: 1 Cat N2: up to 2
Peak DL data rate	N1: 226.7 kbps N2: 282.0 kbps
DL coding type	Tail-Biting Convolutional Code (TBCC)
Physical layer memory requirement	N1: 2112 soft channel bits N2: 7680 soft channel bits
Layer 2 memory requirement	4000 bytes

Considering the most computationally demanding baseband functions, NB-IoT devices can be implemented with baseband complexity lower than 30 MIPS.

2.4.3.7 Deployment Flexibility

As stated in Table 2.3, NB-IoT needs a minimum of 2×200 kHz for a stand-alone FDD deployment. The three deployment operation modes for NB-IoT, as shown in Figure 2.7, provide deployment flexibility based on available spectrum.

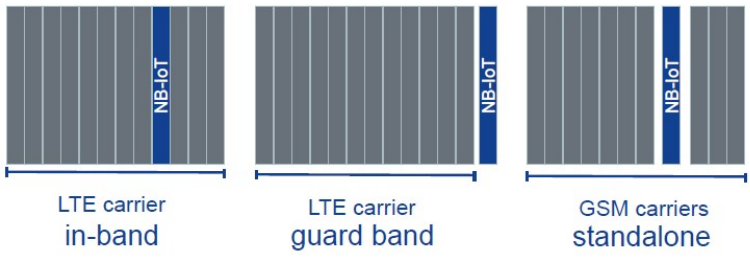

Figure 2.7: NB-IoT operation modes

For in-band operation, at least one LTE PRB is reserved for NB-IoT, although signals must not be transmitted in time-frequency resources reserved for LTE. The sharing of PRBs by NB-IoT and LTE increases the spectrum usage efficiency and increases NB-IoT capacity since more devices

are added to the network. Besides, they can be supported using the same eNB hardware. In guard-band operation mode, each NB-IoT carrier is within the guard-band of LTE. Additionally, LTE subcarrier spacing is used so orthogonality with LTE is maintained. In stand-alone operation, NB-IoT can be used to replace the GSM carriers. This allows the efficient re-farming of GSM carriers for IoT [28].

A consequence of the in-band deployment of NB-IoT is that if one PRB is used for NB-IoT in such cells, the PRB can be used for LTE in other cells. This impacts such deployments in two ways, as depicted in Figure 2.8:

- The sparse deployment of NB-IoT results in a larger area to be covered by each cell;
- The NB-IoT devices that are remote from the serving cell can be potentially within relative proximity to an LTE cell, resulting in strong co-channel interference.

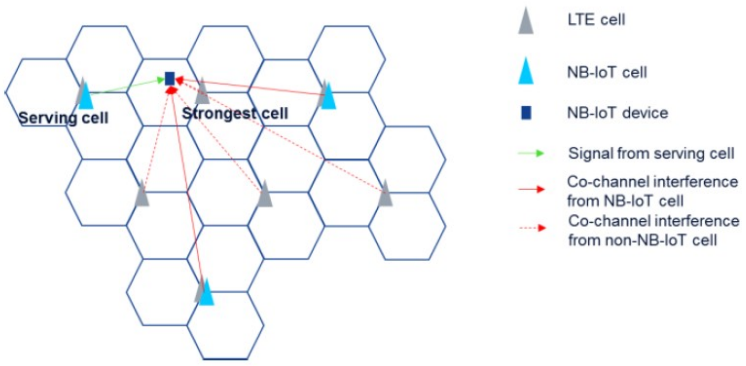

Figure 2.8: In-Band deployment interference [28].

The device is served by the best NB-IoT cell, which is further away from the strongest LTE cell. In this case, the coverage challenge, in addition to path loss from the NB-IoT serving cell, relies on interference from the LTE cell, which will also degrade the connection. This problem may result in a very low Signal-to-Interference-plus-Noise Ratio (SINR) in the NB-IoT device. However, this problem does not exist for guard-band mode.

2.5 Evolution to 5G

Mobile networks have been evolving since their introduction around the 1980s, with about every 10 years a technology shift being introduced towards a new generation. Mobile networks have been evolving from firstly mobile telephony, analog, and digital transmission, and later mobile broadband connectivity to consumers. The introduction of 5G is anticipated around 2020, which will broaden the use cases significantly beyond mobile broadband and consumer-focused services. The targeted usage scenarios for 5G are significantly broader than for earlier mobile network generations, as depicted in Figure 2.9. An example is massive Machine Type Communications (mMTC), which is tailored to enable communications of simple sensor devices that transmit small amounts of delay-tolerant data [3]. This type of communication is the scope of this dissertation.

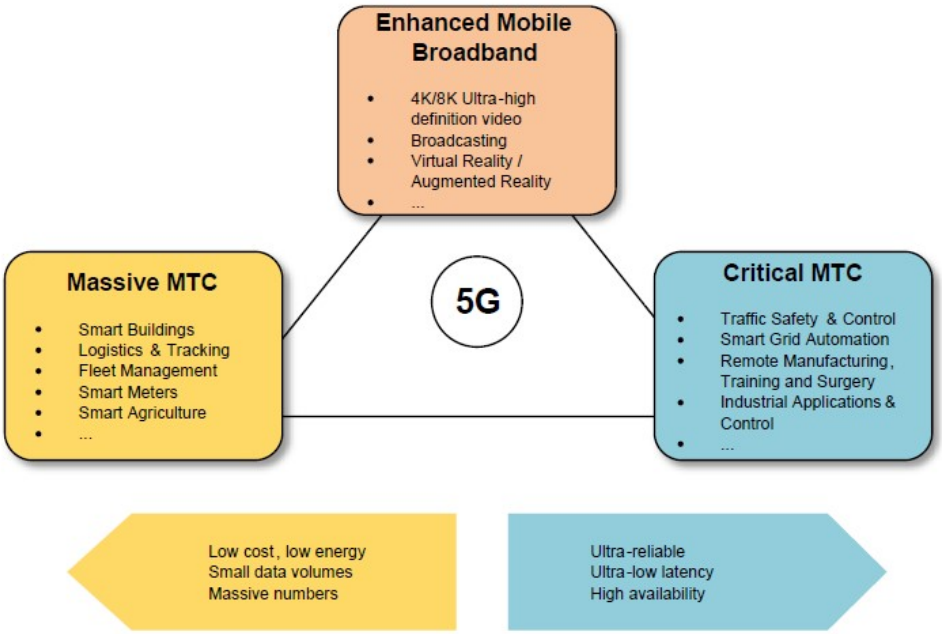

Figure 2.9: 5G use cases.

5G New Radio (NR) is expected to be primarily deployed in dedicated frequency bands that will be assigned to 5G, either in the range above 6 GHz or in new bands below 6 GHz. In the longer run, NR will also migrate to carriers currently used by earlier mobile network standards, such as LTE, where 5G capabilities can be introduced into carriers on which LTE is currently operating. 5G's mMTC requirements defined by 3GPP are presented in Table 2.16, which largely correspond to those of the previous CIoT technologies, where the focus is on extended coverage for low data rates, long device battery lifetime, and scalability to many devices [3].

Table 2.16: 5G mMTC requirements for mMTC [3].

	3GPP Specifications
Coverage	164 dB MCL at 160 bps
System capacity	1.000.000 devices/km^2
UE battery life	10 years battery lifetime (15 years desirable) at 5 Wh sending daily 200 bytes UL 20 bytes DL data MCL 164 dB
Latency	10s for 20 byte application packet UL 164 dB MCL starting the device at the most battery efficient state

5G design for mMTC is a continuation of the CIoT standards LTE-M and NB-IoT. It has been shown that NB-IoT already largely fulfills mMTC 5G requirements [29]. For this reason, 3GPP decided not to specify mMTC solutions in Release 15 [30], but use the evolution of LTE-M and NB-IoT as the baseline of mMTC requirements. Improvements to these technologies include the

early data transmission in the random access procedure to reduce the latency and increase the scalability of CIoT [3].

NB-IoT's deployment flexibility allows an operator to align a CIoT plan with its plans for 5G NR deployment. NB-IoT should be able to operate in-band within an NR carrier in a similar way as if it is deployed in-band within an LTE carrier [3].

2.6 Related Work

In this section, some works regarding the usage and planning of NB-IoT networks are presented.

In [31], the authors present a mathematical model able to predict the throughput or the success probability in a given scenario and the maximum achievable throughput with a certain configuration, by first computing the probability that a device will choose a specific coverage class as a function of distance. They concluded that for NB-IoT to be able to provide good coverage to all devices, the devices should all be configured to belong to the same coverage class.

In [32], a unitary C emulation platform using OAI was developed to verify the effectiveness of existing approaches for UE-specific UL schedulers. It presents a basic UL scheduler to investigate the improvement of the processing time, average delay, and resource utilization.

In [33], a coverage simulation was performed to compare GPRS, NB-IoT, LoRa, and SigFox in a 7800 km^2 area using Telenor's commercial 2G, 3G, and 4G deployment, and determine which of these technologies provides the best coverage for IoT. This study concluded that NB-IoT, due to its MCL of 164 dB, provides the best coverage, in spite of LoRa and SigFox with omnidirectional antennas provide 3dB lower link loss.

In [26], NB-IoT is used for a remote healthcare monitoring system. The realistic performance of NB-IoT is investigated in terms of effective throughput, patient server per cell, and latency for both in-band and stand-alone deployment. A system-level analysis is performed through Monte-Carlo simulations and the performance for Single-sensor Node Design (SND) and Multi-sensor Node Design (MND) is also presented. The authors concluded that for MND there is a significant gain in throughput and the number of patient cells at the cost of increased delay.

In [34], a coverage and capacity analysis for LTE-M and NB-IoT in rural areas was performed for a site-specific network deployment with a Danish operator. This study concluded that LTE-M can provide coverage of 99.9% for outdoor devices, and indoor devices if they are experiencing 10 dB additional loss. However, for deep indoor devices, NB-IoT provides about 95% coverage.

2.7 Summary

In this chapter, the state of the art on CIoT was reviewed. Firstly, public technologies that operate in licensed bands regulated by 3GPP were presented, followed by a brief comparison between them. NB-IoT stands out as the most promising one due to its significantly larger coverage radius

and increased deployment flexibility, by using the narrowest bandwidth, which promotes the co-existence with existing cellular technologies, and three modes of operation, paving the way to be used in scenarios where LTE may not yet be available.

After exploring different CIoT standards and technologies, the most common propagation models for mobile communications were exposed to calculate path losses and, together with the channel BW, determine the desired QoS metrics and meet the required specifications imposed by 3GPP.

Afterward, the aforementioned QoS metrics and requirements were presented, including coverage, latency, battery life, system capacity, device complexity, and deployment flexibility, alongside studies that show how these requirements can be fulfilled.

Thereafter, a short description of the future 5G NR generation of mobile communications was presented, with special emphasis on Machine-To-Machine (M2M) communications and mMTC category, and how the existing technologies such as NB-IoT and LTE-M will evolve towards it. As previously stated, mMTC will be built on top of these technologies, which will facilitate backward compatibility between them and mMTC. NB-IoT upholds as the most promising one by being able to operate in-band within NR carriers as if it was deployed in LTE carriers.

Lastly, related work containing studies conducted to assess NB-IoT's performance regarding coverage, UL scheduling, throughput, and system capacity was presented.

Chapter 3

Developed Theoretical Model

In the previous chapter, the state of the art on CIoT, including QoS metrics, technologies, and standards, as well as a theoretical planning basis for these types of networks were presented. In this chapter, the problem of this dissertation is defined and a solution to address it is proposed. In particular, the proper propagation model to calculate the path losses and predict the power received at each device, to adjust the communication parameters and meet the 3GPP requirements for NB-IoT, is presented. Moreover, the theoretical calculations for throughput and coverage are described.

3.1 Problem Statement

In recent years, IoT applications have grown exponentially, both in the number of connected devices and distance between them. This led to a deprecation of the usage of IEEE 802.11 in these types of networks, as they can no longer answer to the requirements imposed by IoT devices. This dissertation is focused on smart metters, which are characterized by a massive amount of devices in the same area, and typically with low radio coverage, usually in metal cases, inside walls, or even underground, which represent a challenge to IEEE 802.11. For this type of network, CIoT technologies are best-suited, as they can provide long-range communications between a massive number of devices. As stated in Chapter 2, 3GPP proposed three cellular standards to answer IoT requirements, and although they were planned to coexist with existing technologies, such as LTE and GSM, there are still problems between some of them and CIoT.

The main challenges of CIoT include network planning, as new requirements derive from these technologies, such as 1) system capacity, 2) number of connected devices in the same cell, 3) power efficiency and 4) low device complexity for a low cost, while simultaneously providing effective communications regarding Packet Delivery Rate (PDR), latency, throughput, and battery efficiency. These are influenced by communications parameters, including path loss between the devices and the serving cell, interference between CIoT and existing cellular cells, traffic offered by the connected devices, and finally the channel BW for DL and UL communications.

From the network point of view, those QoS metrics rely on the number of repetitions, sleep cycles, Modulation-Coding Scheme (MCS) indexes, number of Resource Unit (RU) for each TB, and the channel's bandwidth. For the UL channels, where Single Carrier Frequency Division Multiple Access (SC-FDMA) is used, the number of tones (Multi/Single tone transmission) must also be considered, as well as SubCarrier-Spacing (SCS), which in this dissertation will be fixed to 15 kHz. These controllable parameters can be tuned according to NB-IoT's requirements previously exposed, to provide a guaranteed QoS to all served users, as depicted in Figure 3.1.

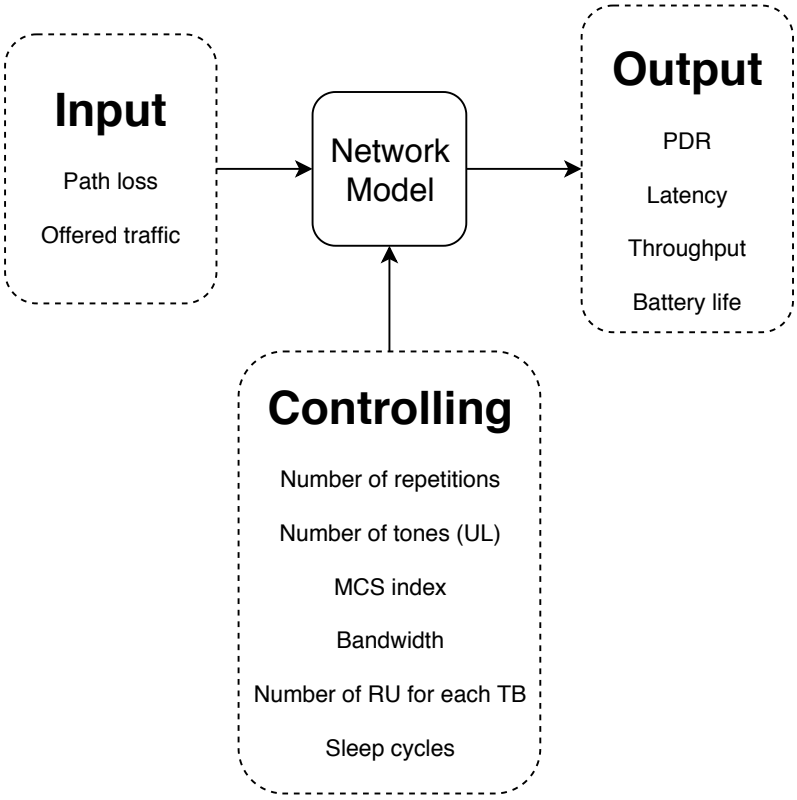

Figure 3.1: Generic network planning model.

Each input, along with the controlled parameters, will influence the output metrics. Regarding the communications channel, as path loss increases, more packets will be dropped, thus decreasing the PDR. This will, in turn, require more repetitions, a more robust Modulation-Coding Scheme (MCS), as well as fewer tones, which will increase the transmission time of the communications and increase battery consumption. Furthermore, large amounts of offered traffic impact the performance of the eNB and its ability to handle requests from the devices, since as more traffic reaches each eNB, the packets held in the transmission queue of each device will increase, therefore increasing the waiting time. Moreover, the channel's BW will mainly affect the throughput, as defined by the Shannon-Hartley theorem, which gives the maximum capacity for the communications channel based on its SNR. The channel BW also affects the PDR, since as the SNR decreases, the Bit Error Ratio (BER) increases.

For the controllable parameters, increasing the transmission power will help to mitigate the effects of path loss, by increasing the SNR, therefore effectively improving the PDR, latency, and throughput. The number of repetitions will further increase the PDR; nevertheless, this will decrease the device's battery efficiency, which will be compensated by the sleep cycles of PSM and eDRX modes.

3.2 System Elements

This work will focus on a specific application: smart meters. These devices are characterized by having a fixed location and usually daily communications. For the sake of simplicity, a single eNB and one smart meter will be considered, as illustrated in Figure 3.2.

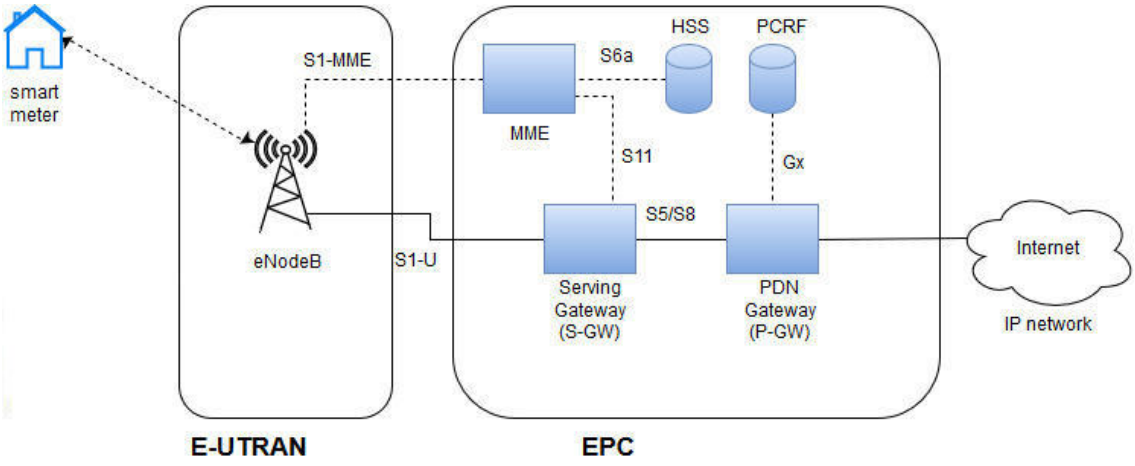

Figure 3.2: Target scenario composed of one eNB and one smart meter.

3.2.1 Smart Meter

The traffic generated by each smart meter will be modeled as an ON/OFF state machine, where the device will only transmit in ON state. During this state, the traffic offered to the system will be modeled as an M/M/1 wait queue, where the packet arrivals are modeled as a Poisson process while the service time assumes an exponential distribution, considering a single server. From the network point of view, the smart meters perform the role of UE.

3.3 NB-IoT Deterministic Link Adaptation Model (NB-DLAM)

To measure network efficiency, the metrics PDR, throughput, latency, and battery performance can be taken into account. These are influenced by the number of repetitions, channel BW, sleep cycle, number of tones, MCS and number of RU of each TB used by the device. As previously stated, for simplicity, subcarrier spacing is set to 15 kHz and the channel BW is set to 180 kHz (both for UL and DL). This work focuses on optimizing PDR by controlling the number of repetitions

and the number of tones, while simultaneously addressing throughput and latency requirements, as depicted in Figure 3.3.

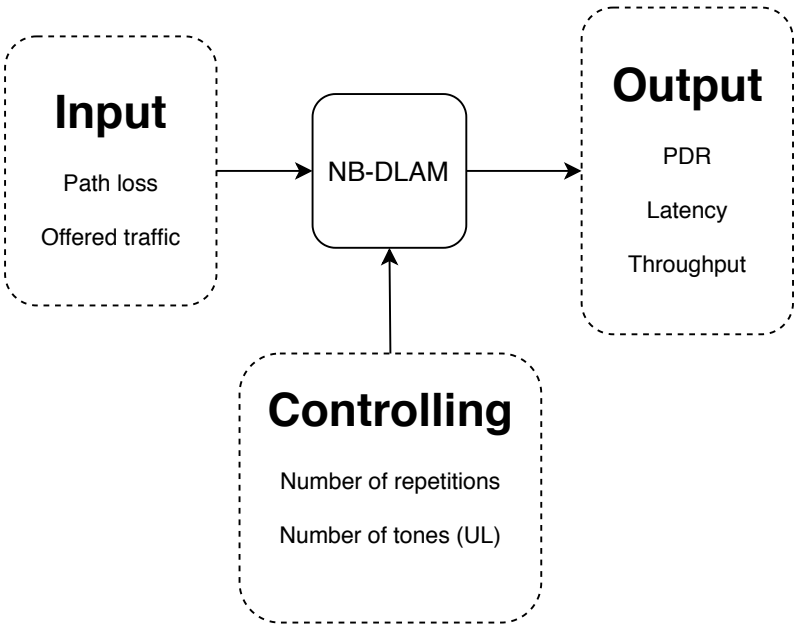

Figure 3.3: Overview of the NB-DLAM.

As stated in the sections before, the increased coverage range of NB-IoT comes mainly from the repetitions of the same packet, which increases the probability that it will be received correctly. As such it is crucial that each UE has the right amount of repetitions configured, keeping in mind that as higher this number is, the longer it will take to send a packet, thus having a direct impact on the communications' latency, achieved throughput, as well as battery life.

As depicted in Figure 3.4, NB-DLAM first validates the NB-IoT restriction on the MCL, which sets a target SNR (SNR_{target}); if the estimated SNR is bellow SNR_{target}, the user is considered out of coverage and is disconnected. After this requirement is met, the number of repetitions and tones are adjusted to ensure a minimum PDR (PDR_{target}). If no suitable configurations are found, the user is disconnected. Lastly, when the previous restrictions are met, transmission time and throughput requirements are validated. When the necessary conditions are met, the user is configured accordingly; otherwise, the user is considered out of coverage, and is disconnected from the serving eNB.

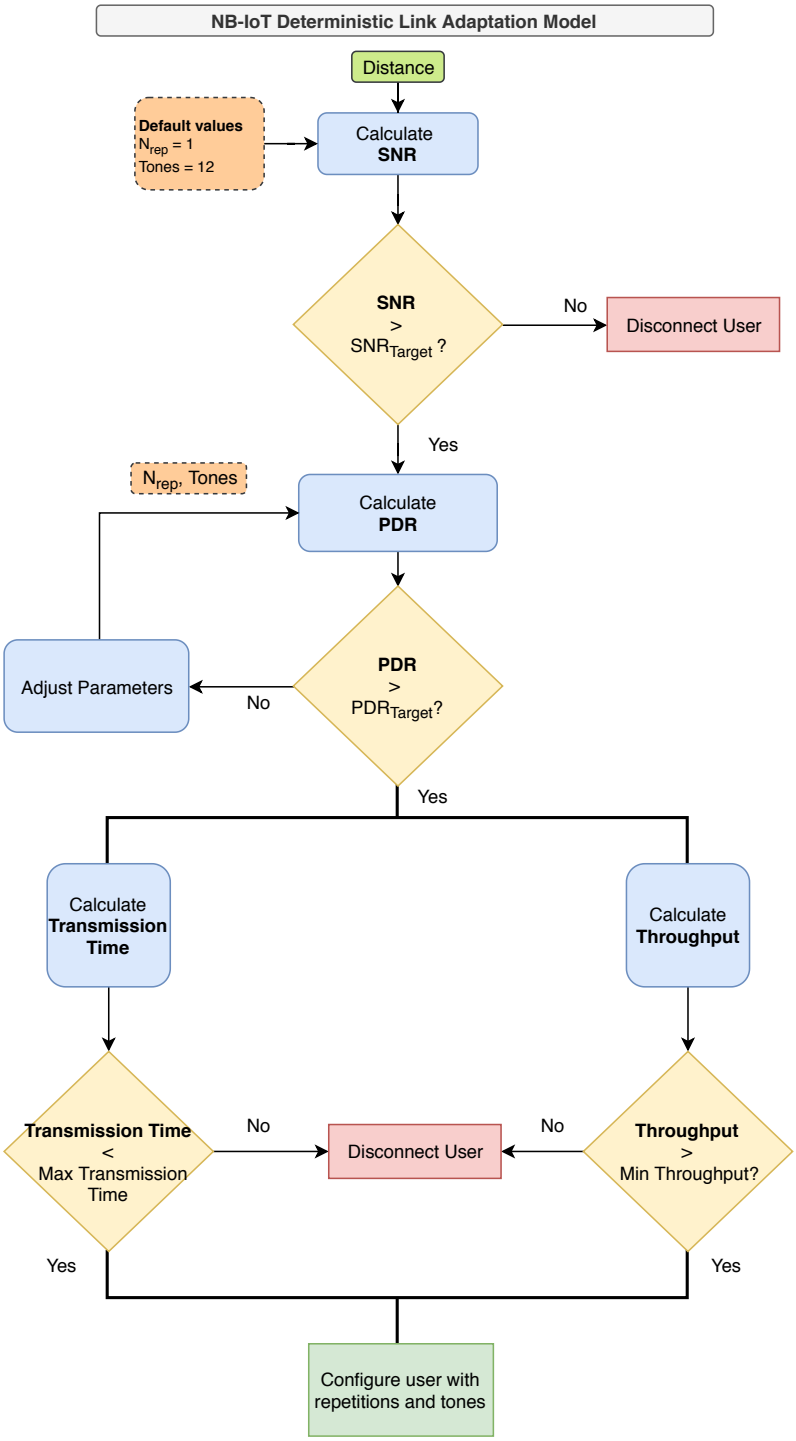

Figure 3.4: NB-DLAM overview.

3.3.1 SNR

To correctly estimate the parameters a terminal needs, it is essential to accurately calculate the link's SNR. As a first step, NB-DLAM calculates the path loss (P_{loss}) experienced by the user at a distance (d), taking into account the link's frequency (f). For that, Log-Distance Path Loss Model,

which is represented in Equation 3.1, is used.

$$P_{lossdB} = 20 \times \log_{10}\left(\frac{4 \times \pi \times d_0}{\lambda}\right) + \gamma \times \log_{10}\left(\frac{d}{d_0}\right) \tag{3.1}$$

where $\lambda = \frac{c}{f}$ ($c = 3E8$) is the link's wavelength and the path loss exponent, γ, can be adjusted for each situation. For the results presented in this work, γ is set to 2, which is equivalent to the Friis propagation model. With this, the power received by each UE and eNB, in DL and UL, respectively, can be calculated using Equation 3.2.

$$P_{rx}(P_{tx}, d)_{dB} = P_{tx} - P_{loss}(d) \tag{3.2}$$

For this theoretical model, Additive White Gaussian Noise (AWGN) was considered when calculating the SNR, considering thermal noise power $N0_{dB} = -174$ dBm.

With this, the transmission power spectral density and noise power spectral density were calculated with Equation 3.3 and Equation 3.4, respectively. These values will be used to calculate the SNR, using Equation 3.5.

$$TxSpectralDensity = \frac{P_{rx}}{BW} \tag{3.3}$$

$$NoiseSpectralDensity = N0 \times NoiseFigure_{watts} \tag{3.4}$$

$$SNR = \frac{TxSpectralDensity}{NoiseSpectralDensity} \tag{3.5}$$

As stated in the previous section, NB-IoT MCL sets a target SNR, that can be calculated with Equation 3.6 and Equation 3.7.

$$EffectiveNoise = 10 \times log_{10}(BW) - N0_{dB} \tag{3.6}$$

$$SNR_{target} = P_{tx} - EffectiveNoise - MCL \tag{3.7}$$

A good calculation of SNR is crucial because it is the main building block of this model. SNR is used to calculate the PDR, which in turn results in the number of repetitions required, and hence the latency and throughput obtained.

3.3.2 Packet Delivery Rate (PDR)

Due to NB-IoT's repetitions-based transmission scheme, the receiver can aggregate all the repetitions of a packet to improve it's overall quality, thus decreasing the error probability. Following

this analysis, the resulting SNR is the sum of the SNR values of each repetition at the receiver, therefore Equation 3.8 naturally arises for the error calculations.

$$SNR(N_{rep}) = \sum_{i=1}^{N_{rep}} (SNR) = SNR \times N_{rep} \tag{3.8}$$

As stated before, each packet is divided into several TB. For each TB, a 24-bit Cyclic Redundancy Check (CRC) is attached and mapped over several RU (N_{ru}), as represented in Figure 3.5. Thereafter, this combination is encoded, with Turbo Coding, and the rate matched according to the used N_{ru} and the number of RE available per RU (Re_{ru}), as depicted in Figure 3.6.

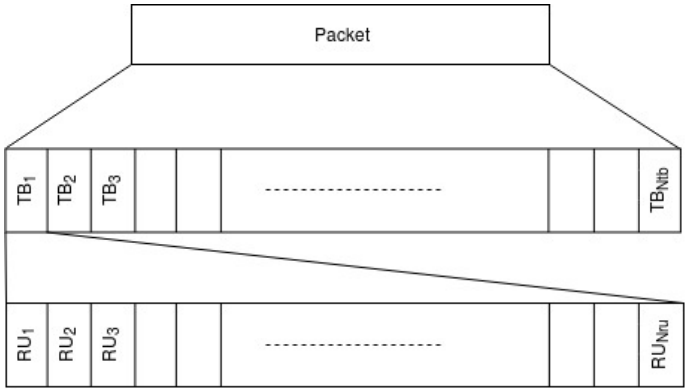

Figure 3.5: Packet division into TB's and RU's.

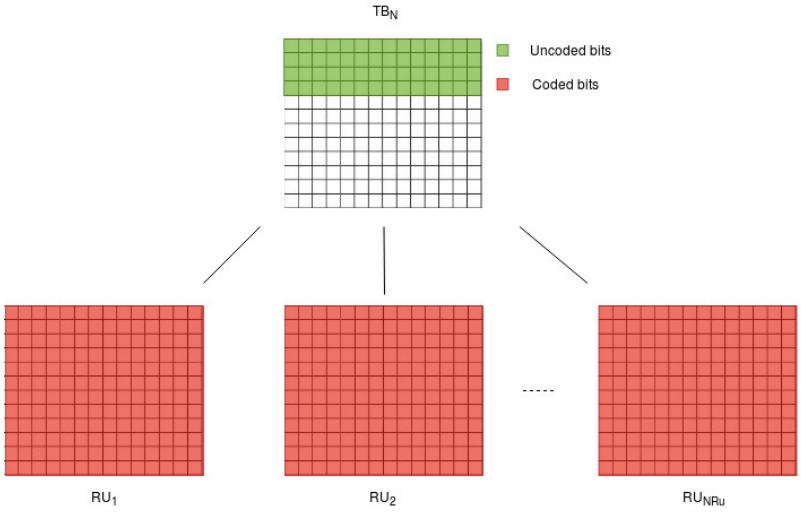

Figure 3.6: TB mapping into RU's.

Finally, taking into account the RU BW, which depends on the number of tones used, as represented in Figure 3.7, and the SCS fixed at 15 kHz, the effective bandwidth is given by Equation 3.9.

$$BW = SCS \times Tones = 15kHz \times Tones, Tones \in [12,6,3,2,1] \tag{3.9}$$

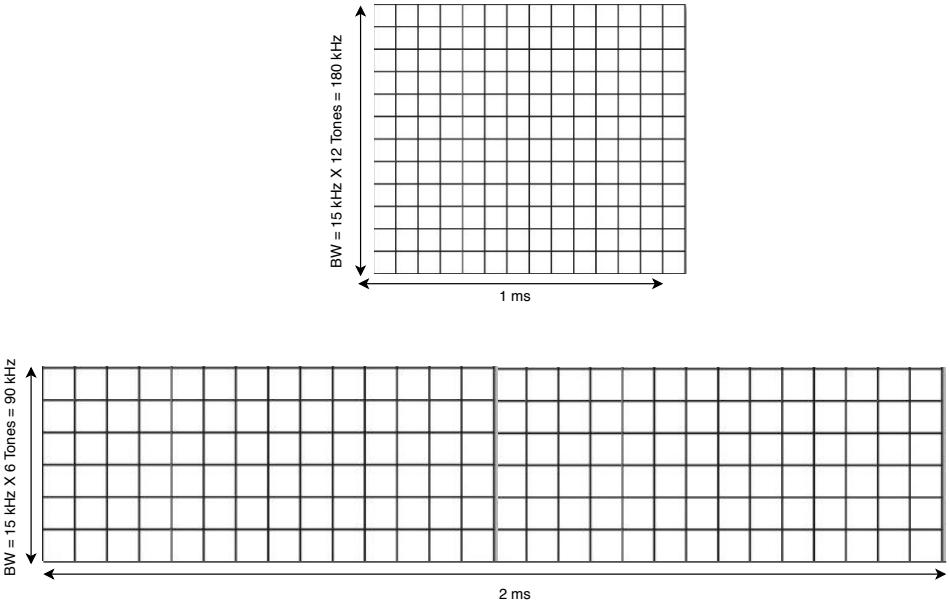

Figure 3.7: RU's bandwidth used with tones.

As the maximum number of tones is 12, which is used for devices in good coverage scenarios that result in the highest BW possible (180 kHz), Equation 3.9 can be rewritten as Equation 3.10, where f is the frequency factor that will be used to improve the SNR.

$$BW = \frac{180kHz}{f}, f = \frac{12}{Tones}, f \in [1,2,4,6,12] \tag{3.10}$$

This means that the final SNR to be used as a basis to calculate the PDR is given by Equation 3.11.

$$SNR_f = SNR \times N_{rep} \times f \tag{3.11}$$

After the SNR is calculated, values for Bit Error Ratio (BER), for QPSK modulation, which uses $M = 4$ symbols, can be obtained, as shown in Equation 3.12.

$$BER = \frac{2}{k} \times Q(\sqrt{2 \times SNR_f} \times \sin(\frac{\pi}{M})); \tag{3.12}$$

To calculate the number of bits transmitted, and based on that, the Packet Error Ratio (PER) and PDR, the coding rate should be determined, according to the coding depicted in Figure 3.6. So, the coding scheme is defined as $k = TBs + CRC$ information bits, represented in green in Figure 3.6, and $n = NRu \times Re_{ru} \times k_{modulation}$ encoded bits, represented in red, where $k_{modulation}$ represents the number of bits used in the modulation scheme ($k_{qpsk} = 2$ for QPSK, which is used throughout NB-DLAM), defined in Equation 3.13.

$$Coding_{rate} = \frac{TBs + CRC}{N_{ru} \times Re_{ru} \times k_{qpsk}} \tag{3.13}$$

As such, the Transport Block size (TBs) of each TB is defined by both the MCS index and the N_{ru} used as defined in Figure 3.8 for NPUSCH. For the NPDSCH channel, the TBs values are the same, except that the maximum TBs is 680 bits. For the TBs values presented in Figure 3.8, the corresponding coding rates for NPUSCH and NPDSCH are found in Figure 3.9a and Figure 3.9b, respectively.

	Number of RUs (N_{RU})							
TBS (I_{TBS})	1	2	3	4	5	6	8	10
0	16	32	56	88	120	152	208	256
1	24	56	88	144	176	208	256	344
2	32	72	144	176	208	256	328	424
3	40	104	176	208	256	328	440	568
4	56	120	208	256	328	408	552	696
5	72	144	224	328	424	504	680	872
6	88	176	256	392	504	600	808	1000
7	104	224	328	472	584	712	1000	Not used
8	120	256	392	536	680	808	Not used	Not used
9	136	296	456	616	776	936	Not used	Not used
10	144	328	504	680	872	1000	Not used	Not used
11	176	376	584	776	1000	Not used	Not used	Not used
12	208	440	680	1000	Not used	Not used	Not used	Not used

Figure 3.8: TBS for NPUSCH [3].

Considering the BER, the Packet Error Ratio (PER) can be calculated. As explained, the user can aggregate all the repetitions, increasing the SNR, so the number of repetitions will not be considered when calculating the PER and PDR, as this is already expressed in the SNR. Furthermore, using coding increases the packet size as shown in Equation 3.14, which is then used to calculate PER and PDR with Equation 3.15 and Equation 3.16, respectively.

$$PacketSize_{cr} = \frac{PacketSize}{CodingRate} \tag{3.14}$$

$$PER = 1 - (1 - BER)^{PacketSize_{cr}} \tag{3.15}$$

$$PDR = 1 - PER \tag{3.16}$$

NPUSCH TB size index	Number of RUs							
	1	2	3	4	5	6	8	10
0	0.14	0.10	0.09	0.10	0.10	0.10	0.10	0.10
1	0.17	0.14	0.13	0.15	0.14	0.13	0.12	0.13
2	0.19	0.17	0.19	0.17	0.16	0.16	0.15	0.16
3	0.22	0.22	0.23	0.20	0.19	0.20	0.20	0.21
4	0.28	0.25	0.27	0.24	0.24	0.25	0.25	0.25
5	0.33	0.29	0.29	0.31	0.31	0.31	0.31	0.31
6	0.39	0.35	0.32	0.36	0.37	0.36	0.36	0.36
7	0.44	0.43	0.41	0.43	0.42	0.43	0.44	Not used
8	0.50	0.49	0.48	0.49	0.49	0.48	Not used	Not used
9	0.56	0.56	0.56	0.56	0.56	0.56	Not used	Not used
10	0.58	0.61	0.61	0.61	0.62	0.59	Not used	Not used
11	0.69	0.69	0.70	0.69	0.71	Not used	Not used	Not used
12	0.81	0.81	0.81	0.89	Not used	Not used	Not used	Not used

(a) Coding rates used in NPUSCH [3].

NPDSCH TB Size Index	Number of NPDSCH Subframes (N_{SF})							
	1	2	3	4	5	6	8	10
0	0.13	0.09	0.09	0.09	0.09	0.10	0.10	0.09
1	0.16	0.13	0.12	0.14	0.13	0.13	0.12	0.12
2	0.18	0.16	0.18	0.16	0.15	0.15	0.14	0.15
3	0.21	0.21	0.22	0.19	0.18	0.19	0.19	0.19
4	0.26	0.24	0.25	0.23	0.23	0.24	0.24	0.23
5	0.32	0.28	0.27	0.29	0.29	0.29	0.29	Not used
6	0.37	0.33	0.31	0.34	0.35	0.34	Not used	Not used
7	0.42	0.41	0.39	0.41	0.40	0.39	Not used	Not used
8	0.47	0.46	0.46	0.46	0.46	Not used	Not used	Not used
9	0.53	0.53	0.53	0.53	Not used	Not used	Not used	Not used
10	0.55	0.58	0.58	0.58	Not used	Not used	Not used	Not used
11	0.66	0.66	0.67	Not used	Not used	Not used	Not used	Not used
12	0.76	0.76	0.77	Not used	Not used	Not used	Not used	Not used

(b) Coding rates used in NPDSCH [3].

Figure 3.9: Coding rates used.

3.3.3 Transmission Time

As previously explained, each packet is divided into several Transport Blocks (TBs), and each TB is mapped to several Resource Unit (RU) (N_{ru}). In a packet there are $N_{tb} = \frac{PacketSize}{TB_{size}}$ TBs, and each RU's transmission time (t_{ru}) depends on the number of tones used, as depicted in Figure 3.10. Decreasing the number of tones will increase transmission time, as the UE will take longer to transmit the same number of bits, hence the transmission time (t_{ru}) according to f is given by Equation 3.17.

$$t_{ru} = 1ms \times f, t_{ru} \in [1,2,4,6,8]ms \tag{3.17}$$

Thus, the *TransmissionTime* can be estimated beforehand, and a lower bound can be calculated with Equation 3.18.

$$TransmissionTime = N_{ru} \times N_{tb} \times N_{rep} \times t_{ru} \tag{3.18}$$

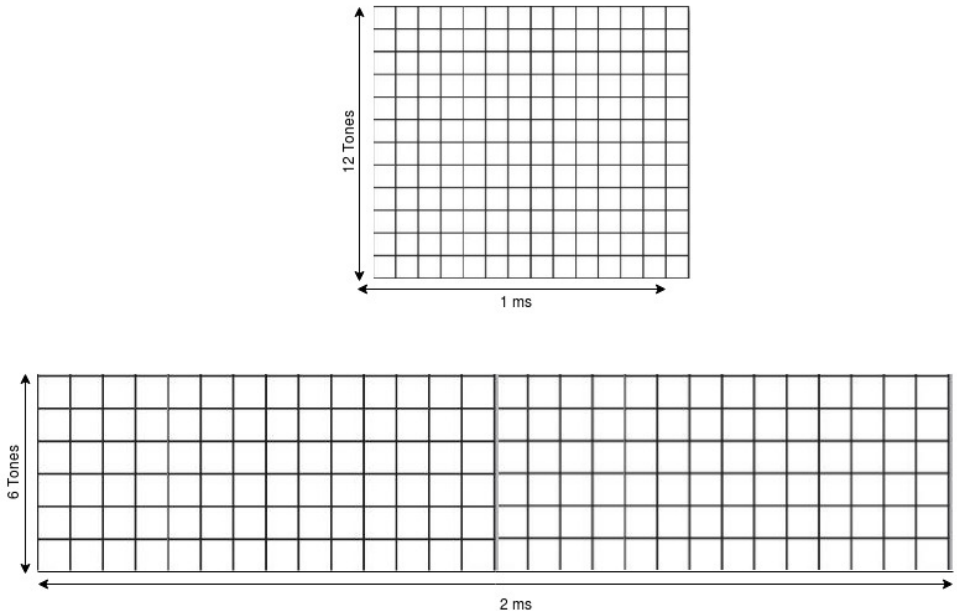

Figure 3.10: RU's transmission time with tones.

3.3.4 Throughput

In NB-IoT, each data packet is segmented into one or more TB, where each one is transmitted at a time. NB-IoT allocates the subframe indexes to each user on the NPDSCH channel.

Considering the NB-IoT's subframe structure as depicted in Figure 3.11, and taking into account that a subframe is the smallest allocation unit, this will be used to calculate a theoretical throughput. This allocation unit is named PRB in DL channel and RU in the UL channel. As seen in Figure 3.11, the basic subframe structure is comprised of 14 OFDM symbols, where each symbol is carried over 12 subcarriers. As the modulation used is QPSK, each subcarrier transports 2 bits. This results in $12 subcarriers \times 14 OFDM_{symbols} \times 2 bits = 336$ bits being transported over 1 ms.

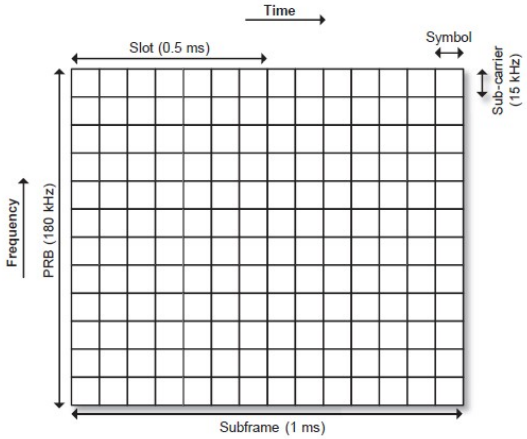

Figure 3.11: Physical Resource Block (PRB).

In the in-band operation mode, some subframes will not be available for NB-IoT, since they are reserved for LTE communications, and thus will be considered invalid subframes. Although the results presented here consider NB-IoT in stand-alone mode, the model is ready to deal with invalid subframes. Following the frame format depicted in Figure 3.12, valid subframes will be allocated to users, considering the bits transmitted in each subframe, until $PacketSize \times Repetitions$ bits are transmitted, meaning that for more repetitions, more subframes will be needed, increasing latency.

Figure 3.12: Frame format.

As subframe 0 is reserved for the DL control channel NPBCH, subframe 5 for NPSS, and subframe 9 for Narrowband Secondary Synchronization Signal (NSSS), they are invalid subframes, and will not be allocated to any user for the NPDSCH channel. For the Narrowband Reference Signal (NRS) channel there are three important rules to take into account:

- In all operation modes, NRS is present in subframes 0 and 4, as well as in subframe 9 not containing NSSS;
- In stand-alone and guard-band modes, NRS is also present in subframes 1 and 3;
- In all operation modes, NRS is present in all valid NB-IoT DL subframes.

As the last rule states, the NRS signal is present in all valid DL subframes, so the bit allocation depicted in Figure 3.13 needs to be considered as it will reduce the number of usable bits in a subframe, and is dependent on the number of antenna ports that are used.

As previously stated, each valid subframe is capable of carrying at most 336 bits. Considering that NRS signal is carried in all DL subframes, mapped to certain subcarriers in the last OFDM symbols in every slot, the number of usable bits will be $336 - NumberOfPorts \times NumberOfSubcarriers \times NumberOfSymbols$.

Although other configurations would be possible, this model assumes that NRS is carried in subcarriers 0, 3, 6, 9, as depicted in Figure 3.13, and only one antenna port is used, that is, in symbols 6 and 13, resulting in $336 - 1 \times 4 \times 2 = 328$ bits over 1 ms. This means that if a user sends 680 bits with 1 repetition, two subframes would need to be reserved, hence, 2 ms of transmission time, thus having a maximum transmission throughput of $\frac{680}{2ms} = 340$ kbit/s, resulting in the example subframe allocation depicted in Figure 3.14. In turn, considering the allocation depicted in Figure 3.15, the transmission would span over 3 ms, dropping the throughput to $\frac{680}{3ms} =$ 226.67 kbit/s.

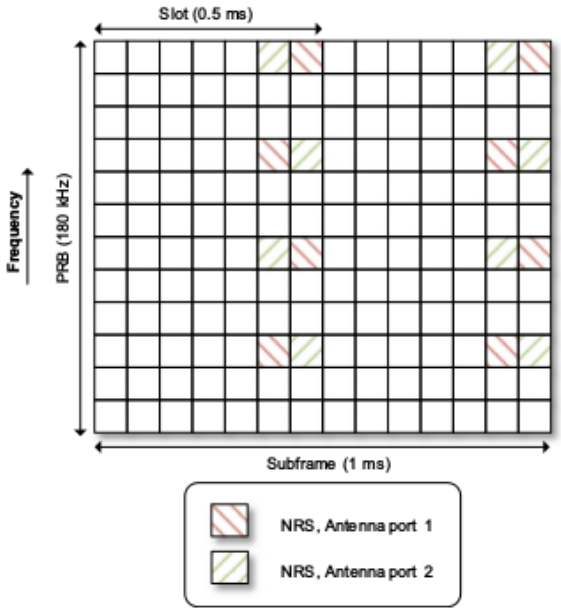

Figure 3.13: NRS subframe.

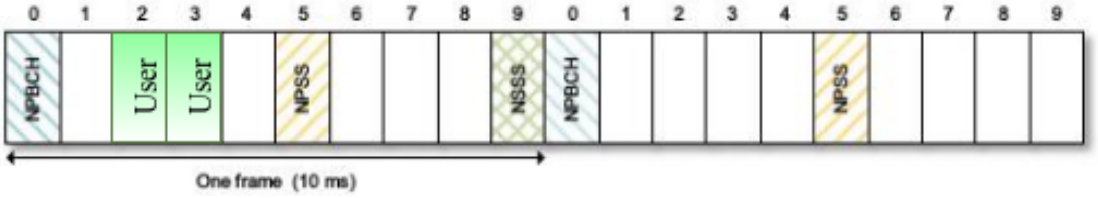

Figure 3.14: Example of subframe allocation.

Figure 3.15: Example 2 of subframe allocation.

In the previous examples, only 1 repetition was considered, but if more are needed, a single repetition would be considered and the time it takes to transmit all of the repetitions would be taken into account. This results in a drop in throughput and an increase in latency. As seen in Figure 3.16, the same packet with 680 bits is to be transmitted, but with 2 repetitions, with subframes 6, 7, 8 from frame 1, and subframe 1 from frame 2 being allocated. This results in $\frac{680}{6ms} = 113.33$ kbits/s. Generically, this can be summarized by Equation 3.19 and Equation 3.20, considering the subframe allocation for each user, accounting for the last subframe allocated in the last frame used and the first subframe allocated in the first frame used.

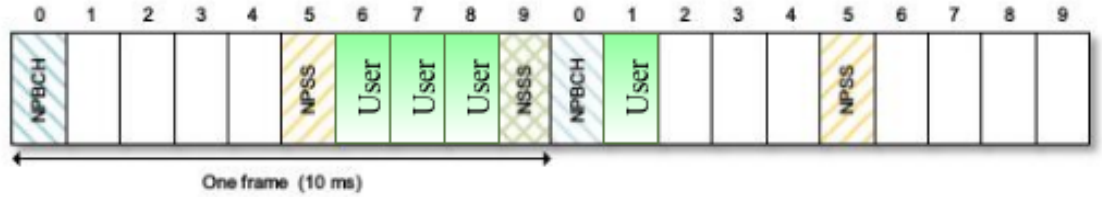

Figure 3.16: Example 3 of subframe allocation.

$$TransmissionTime = [(LastFrame \times 10 + LastSubframe) - (FirstFrame \times 10 + FirstSubframe) + 1] \times 1ms(s) \quad (3.19)$$

$$R_1 = \frac{PacketSize}{TransmissionTime}(bits/s) \quad (3.20)$$

Taking into account Equation 3.20 and the information provided in the previous chapter, where estimations for BER were given and coding rate values were presented, the final throughput can be calculate using Equation 3.21.

$$R = R_1 \times Coding_{rate} \times (1 - BER) \quad (3.21)$$

3.3.5 Channel capacity

To obtain the maximum throughput for a given communications channel, the Shannon-Hartley theorem was used, as represented in Equation 3.22.

$$C = B \times \log_2(1 + SNR) \quad (3.22)$$

This channel capacity is used together with the throughput calculations explained in Subsection 3.3.4, where the final result for the transmitted throughput is given by Equation 3.23.

$$R_{transmitted} = min(C, R) \quad (3.23)$$

3.3.6 Scheduling

When dealing with multiple users, some kind of scheduling algorithm must be implemented to fairly deal with the demand. This model uses a simple round-robin scheduling algorithm where a valid subframe, which represents an RU of one TB of the packet to be transmitted, is assigned to each user at each round until it has nothing else to transmit.

In the example seen in Figure 3.17, two users need to transmit a 680 bits packet each, where User 1 requires 2 repetitions, and User 2 requires only 1 repetition. This model allocates 1 subframe for each user iteratively, until both users transmit all data.

Figure 3.17: Example of subframe scheduling.

From the given subframe allocation, and using the results from Subsection 3.3.4, we get:

- User 1: $\frac{680}{7ms} = 97$ kbits/s
- User 2: $\frac{680}{3ms} = 226.67$ kbits/s

3.3.7 Parameters adjustment

As it has been explained throughout this chapter, it is crucial to find an optimal configuration for the UE regarding the number of repetitions and tones used in the UL channel, as this will have a direct impact on the QoS metrics PDR, throughput, and transmission time.

As seen in Figure 3.4, all users will be assigned with the default configurations $N_{rep} = 1$ and $Tones = 12$, since this will not affect their coverage, as demonstrated in Subsection 3.3.2. These configurations result in $SNR_f = SNR \times 1 \times 1$.

As explained in Subsection 3.3.2, increasing the number of repetitions improves the PDR with the drawback of increasing the transmission time of one packet, as seen in Subsection 3.3.3; this will degrade the resulting throughput, as depicted in Subsection 3.3.4. The decrease in the number of tones used will reduce the BW used (cf. Figure 3.7), thus increasing the resulting SNR and coverage. This reduction will degrade the transmission time, since it will take longer to transmit the same number of bits, as depicted in Figure 3.10.

NB-DLAM tries to keep a minimum PDR (PDR_{target}) to ensure reliable communications, while ensuring target requirements for SNR, throughput, and transmission time, as follows:

$$\begin{cases} PDR_{target} >= 99\% \\ Throughput >= 160 bits/s \\ TransmissionTime <= 10s \end{cases}$$

As the number of repetitions will have a higher impact on the resulting SNR (SNR_f), the proposed model first decreases the number of tones, and if no suitable configuration is found, this is reset to 12, and the number of repetitions is increased. This process is repeated, until the PDR requirement is met, or the maximum number of repetitions is reached (128 in UL).

As a simplification, the MCS index and number of RU, N_{ru}, are fixed to 12 and 1, respectively. Changing these values would decrease the coding rate, making the communication more robust to errors, introducing coding gain, decreasing the BER, and further increasing coverage.

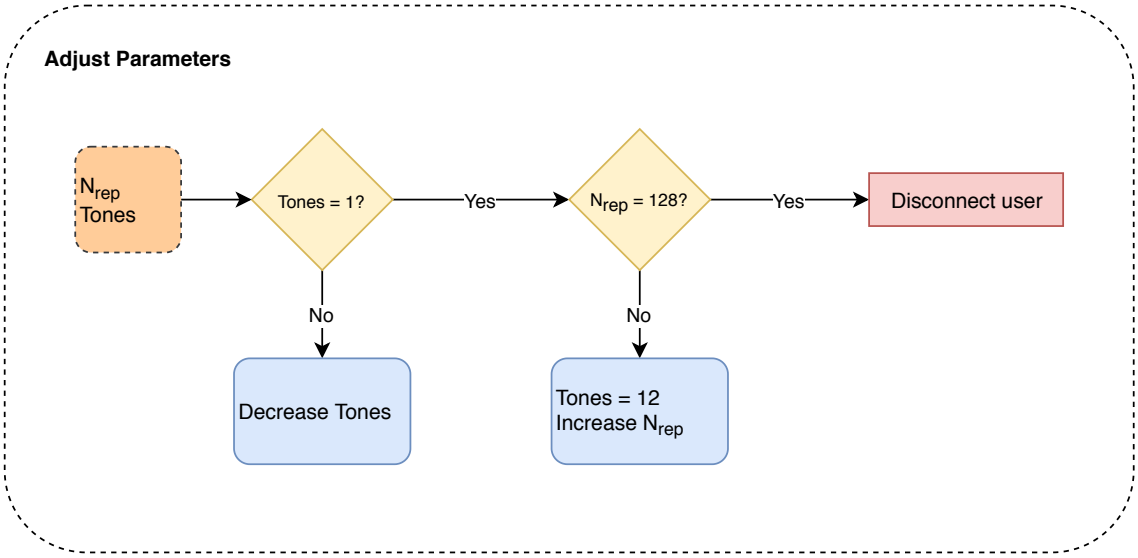

Figure 3.18: Adjust parameters.

3.4 Summary

In this chapter, the problem statement was presented, introducing the need for a model that can meet the strict NB-IoT requirements by leveraging the tools provided by this technology. Thereafter, an NB-IoT theoretical model was proposed, which takes into account the theoretical concepts presented in Chapter 2 to achieve the NB-IoT requirements.

Chapter 4

Validation of the Developed Theoretical Model

In this chapter, the validation of the proposed model, NB-DLAM is presented, including the simulation setup, changes made to the used simulator to enable proper validation, the simulation scenario, and how the desired metrics were measured. Lastly, the model's theoretical results are presented and compared against simulation results.

4.1 Simulation Setup

To validate NB-DLAM, the NB-IoT ns-3 implementation[1] developed by IMEC-IDLab was used. To the best of our knowledge, it was, at the time of writing this dissertation, the most stable open-source NB-IoT simulator, supporting both repetitions and tones [12]. More specifically the *repetition_coverage* branch[2] was used as it provides the tools to validate the theoretical model proposed by this dissertation. The ns-3 simulator is widely accepted within the scientific community due to its accuracy, particularly in wireless networks. This paves the way for a proper validation.

To validate the model, an ns-3 script was developed following the network architecture depicted in Figure 4.1. An NB-IoT UE equipment attached to an eNB through a link affected by Log Distance Propagation Loss Model were part of the simulation scenario. Since ns-3 does not have a Rayleigh fading model, Nakagami Propagation Loss Model was used, setting all three constants $m0$, $m1$, $m2$ to 1, which is equivalent to Rayleigh fading. The eNB was then connected to a remote host through an IPv4 Point to Point connection with 100 Gb/s of throughput and 1ms of delay.

To obtain measures of SNR in relation to distance, a single UE was placed at the same position as the eNB and then moved in a straight line, using the Constant Velocity Mobility Model.

[1] https://github.com/imec-idlab/NB-IoT
[2] https://github.com/imec-idlab/NB-IoT/tree/repetition_coverage

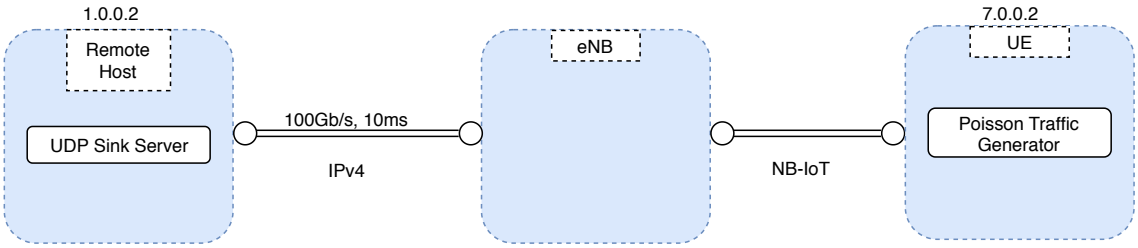

Figure 4.1: Network architecture used in ns-3.

The starting and finishing distances and simulation time were passed through command line arguments, which were used to calculate the velocity required by the mobility model, as showed in Equation 4.1,

$$velocity = \frac{finish - start}{simTime} \tag{4.1}$$

where $finish$ and $start$ are the finishing and starting positions respectively, and $simTime$ is the simulation time. This guarantees that the user runs through all required distances, within the simulation. SNR values were then obtained with a $PhyStatsCalculator$ object and stored in a file, where a line with an entry for each simulation instant and the corresponding SNR value was included. This file was then processed by a python script, in charge of reading the SNR and the simulation instant (t) values and calculating the respective distance with Equation 4.2, thus obtaining the relation between SNR and distance.

$$distance = start + t \times velocity \tag{4.2}$$

To obtain results for the PDR, throughput, and delay, for each distance, a simulation was run for all distances with a stationary user, generating UL traffic and measuring the bytes sent and received, as well as the transmission delay using the $RadioBearerStatsCalculator$ of the $LteHelper$, which stores the Radio-Link Control (RLC) statistics in a file. In this file, some relevant values were stored including $TxBytes$, $RxBytes$, and $delay$, which were used to calculate PDR, $TransmissionTime$, and $Throughput$ as shown in Equation 4.3, Equation 4.4, and Equation 4.5.

$$PDR = \frac{RxBytes}{TxBytes} \tag{4.3}$$

$$TransmissionTime = delay \tag{4.4}$$

$$Throughput = RxBytes \tag{4.5}$$

The main device configurations used for both the eNB and UE can be found in Table 4.1 and Table 4.2, respectively. The UL frequency was set using the 3650 E-UTRA Absolute Radio Frequency Channel Number (EARFCN) that corresponds to the GSM band 8, named 900 GSM,

for which 945 MHz was used as the carrier frequency (f_c).

For the Log Distance Propagation Loss Model, the attributes $ReferenceDistance$ and $ReferenceLoss$ are given by Equation 4.6 and Equation 4.7,

$$ReferenceDistance = 10 \times \lambda \tag{4.6}$$

$$ReferenceLoss = 20 \times \log_{10}\left(\frac{4 \times \pi \times ReferenceDistance}{\lambda}\right) \tag{4.7}$$

where $\lambda = \frac{c}{f_c}$, $c = 3E8$ m/s.

Table 4.1: eNB.

P_{tx}	0 dBm
NoiseFigure	0 dB
Antenna gain	0 dB
Antenna height	30 m
Antenna ports	1

Table 4.2: UE.

P_{tx}	0 dBm
NoiseFigure	0 dB
Device height	0 m
Packet size	1000 bits
Packet rate	1000 packets/s
Antenna gain	0 dB

4.2 Changes in ns-3

When ns-3 uses only deterministic path loss models, such as *LogDistance* or *Friis* propagation models, packet losses are not included, hence it is necessary to use a stochastic path loss model, to introduce fading in the communications channel. To support several types of propagation models, the main ns-3 repository[3] and the experimental NB-IoT repository[4] have a linked list of propagation models, where the power transmitted passes through all of them, to calculate the power received by the endpoint on the receiving side of the channel. Although the stable NB-IoT repository[5] also uses a linked list of propagation models, the changes introduced in the code removed the ability to chain more than one propagation model. As previously explained, this functionality is important to measure PDR. To enable this, Code 4.1 was modified to add a new propagation model at the beginning of the chain of the propagation models, as shown in Code 4.2. This piece of code is located in src/spectrum/model/multi-model-spectrum-channel.cc of the source code.

[3] https://gitlab.com/nsnam/ns-3-dev
[4] https://github.com/TommyPec/ns-3-dev-NB-IOT
[5] https://github.com/imec-idlab/NB-IoT

Code 4.1: Original Code.

```
1 void
2 MultiModelSpectrumChannel::
3 AddPropagationLossModel
4 (Ptr<PropagationLossModel> loss) {
5   NS_LOG_FUNCTION (this << loss);
6   NS_ASSERT(m_propagationLoss == 0);
7   m_propagationLoss = loss;
8 }
```

Code 4.2: Modified code.

```
void
MultiModelSpectrumChannel::
AddPropagationLossModel
(Ptr<PropagationLossModel> loss) {
    NS_LOG_FUNCTION (this << loss);
    loss->SetNext(m_propagationLoss);
    m_propagationLoss = loss;
}
```

Specifically, the changes were made in the highlighted lines; in the original code this line would prevent to add new propagation models, whereas in the modified code, the current propagation model (*m_propagationLoss*) was chained to the new one (*loss*).

Although the ns-3 code was modified in the time domain to support repetitions, there is no way of setting a predefined number of repetitions at the simulation setup and force the UE to use that value throughout the simulation. As this is an important feature required to test the accuracy of the developed model, changes were made to the scheduler used by the ns-3 script, in order to support this feature. The *RrFfMacScheduler* scheduler class was used. The change introduced here was only employed for testing purposes, as it assigns the same repetitions to all users, which might not be desirable in other simulation scenarios. Firstly, a new variable (*m_repetitionNumber*) was added, which defines the number of repetitions that will be attributed to the user, with the respective getters and setters (cf. Code 4.3 and Code 4.4). This variable was used as a new attribute (*Repetitions*) to the *RrFfMacScheduler* scheduler class, as defined in Code 4.5. This attribute was then used when the scheduler was called to send the UL Downlink Control Information (DCI) control message, where the number of user's repetitions was set. The code snippets presented can be found in the src/lte/model/rr-ff-mac-scheduler.cc file.

Code 4.3: *Repetitions* getter.

```
1 uint32_t
2 RrFfMacScheduler::
3 GetRepetitions() const {
4   return m_repetitionNumber;
5 }
```

Code 4.4: *Repetitions* setter.

```
void
RrFfMacScheduler::
SetRepetitions(uint32_t repetitions) {
  m_repetitionNumber = repetitions;
}
```

Code 4.5: RrFfMacScheduler new attribute; *Repetitions*.

```
.AddAttribute("Repetitions",
    "Number of fixed repetitions to use in uplink [default: 1].",
    UintegerValue(1),
    MakeUintegerAccessor(&RrFfMacScheduler::SetRepetitions,
                         &RrFfMacScheduler::GetRepetitions),
                         MakeUintegerChecker<uint32_t>(1, 128))
```

Code 4.6: Original scheduler for repetitions.

```
1 ...
2 if (REPEAT){
3     uldci.m_repetitionNumber =
4         n_times;
5     if (EXHAUSTIVE || ANALYTICAL)
6     ...
7 }
```

Code 4.7: Modified scheduler for repetitions.

```
...
if (REPEAT){
    uldci.m_repetitionNumber =
        m_repetitionNumber;
    if (EXHAUSTIVE || ANALYTICAL)
    ...
}
```

Since the number of repetitions was defined in the UL DCI message (*uldci.m_repetitionNumber*), this value is then overwritten by *m_repetitionNumber*, which is highlighted in Code 4.7. Set beforehand, during setup, forcing every user to share the same number of repetitions.

Lastly, to validate that the effect the number of tones has on the communications' quality, a similar approach was taken. A new variable was added to the *RrFfMacScheduler* (*m_tonesNeeded*), which represents the predefined number of tones that will be assigned by the scheduler. This will be used as a new attribute (*Tones*), as defined in Code 4.8, with the respective getter and setter (cf. Code 4.9 and Code 4.10).

Code 4.8: RrFfMacScheduler new attribute; *Tones*.

```
.AddAttribute("Tones",
              "Number of fixed tones to use in uplink [default: 12].",
              UintegerValue(12),
              MakeUintegerAccessor(&RrFfMacScheduler::SetTones,
                                   &RrFfMacScheduler::GetTones),
              MakeUintegerChecker<uint32_t>(1, 12))
```

Code 4.9: *Tones* getter.

```
uint32_t
RrFfMacScheduler::
GetTones() const{
  return m_tonesNeeded;
}
```

Code 4.10: *Tones* setter.

```
void
RrFfMacScheduler::
SetTones(uint32_t tones){
  m_tonesNeeded = tones;
}
```

After this attribute has been set during setup, with the results taken from the model, its value was assigned to *tonesneeded*, which was used to build the UL DCI message as it is used to define the number tones used. The original code in Code 4.11 was modified as is shown in Code 4.12.

Code 4.11: Original scheduler for tones.

```
...
if (TONE)
    {

        if (tonesneeded == 0)
            ...
    }
```

Code 4.12: Modified scheduler for tones.

```
...
if (TONE)
    {
        tonesneeded = m_tonesNeeded;
        if (tonesneeded == 0)
            ...
    }
```

The highlighted line in Code 4.12 overrides the previously set value for *tonesneeded* with the value of *m_tonesNeeded*. This will be used to define the number of tones used by the UE, as well as its SCS. This UL DCI control message is then processed in the src/lte/model/lte-ue-phy.cc file.

While running the simulations with the changes exposed in this section, an exception was being thrown for *Tones* $<= 3$. This was due to a bug found in the src/lte/model/lte-spectrum-phy.cc file. As the number of tones is reduced, the transmission time increases accordingly, as explained in Subsection 3.3.3. With *Tones* $<= 3$, the transmission time of the data frame would overlap with the transmission time of a control frame. When there was an attempt to transmit this control frame, the state of the device was first checked to confirm whether it was ready to send control frames, in *IDLE* state, or if it still had data to transmit, *TX_DATA* state, as shown in Code 4.13.

Code 4.13: SRS control changes.

```
...
 case TX_DATA:
    // Debug message
  case IDLE:
    ...
    ChangeState(TX_UL_SRS);
    m_channel->StartTx(txParams);
 ...
```

As can be seen, inside the *TX_DATA* case, there is no *break* statement, which in the C language causes the *IDLE* case to execute. This means that the device would attempt to transmit the control message, regardless if there was data to be sent or not, which would, later on, cause the exception "*assert failed. cond="m_txPacketBurst == 0""* to be thrown. To fix this, the missing *break* statement was added as shown in the highlighted line in Code 4.14.

Code 4.14: SRS control changes

```
...
 case TX_DATA:
    // Debug message
    break;
  case IDLE:
    ...
    ChangeState(TX_UL_SRS);
    m_channel->StartTx(txParams);
 ...
```

4.3 Model results

As this dissertation is focused on improving the performance of the communications in the direction from the UEs (smart metters) to the eNB through the use of repetitions and tones, the results presented in this section cover mostly the UL channel, although the same results apply to the DL channel, since the conditions are identical (i.e., same transmission power, same noise, and a single user, which ensures there is no interference in UL). Furthermore, the main difference between UL and DL in the aforementioned conditions is the number of repetitions in each channel, as the DL channel (NPDSCH) has a much greater number (2048) than the UL (128) channel (NPUSCH). This increases even further the DL coverage.

For the specific type of application that this dissertation is focused on, the transmission time is not a relevant aspect, as smart metters are expected to send few packets in a course of a day, so the maximum admittable transmission time considered is the 10s claimed by the NB-IoT requirements. Moreover, for the reasons previously stated, throughput is also not relevant, with the minimum target of NB-IoT being 160 bits/s, which is considered in this dissertation.

Using the results from Equation 3.2 and Equation 3.5, the theoretical SNR can be found in Figure 4.2. Although the aforementioned equations represent the SNR in watts, for simplicity of analysis the results depicted in the following figures are in dB.

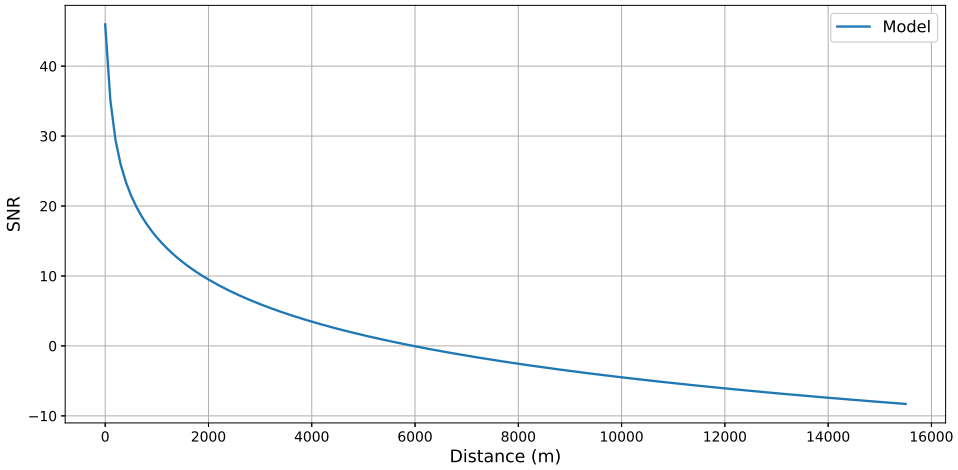

Figure 4.2: SNR as a function of distance, which was obtained using NB-DLAM.

Using the previous SNR results and Equation 3.12, Equation 3.15 and Equation 3.16, PDR versus distance was calculated considering the different repetitions available for the NPUSCH channel, depicted in Figure 4.3, and the number of tones, depicted in Figure 4.4. The results presented for each configuration (*Repetitions* or *Tones*) assume that the parameter that is not under study is set to its default value, i.e., for Figure 4.3, $Tones = 12$, while for Figure 4.4, $Repetitions = 1$.

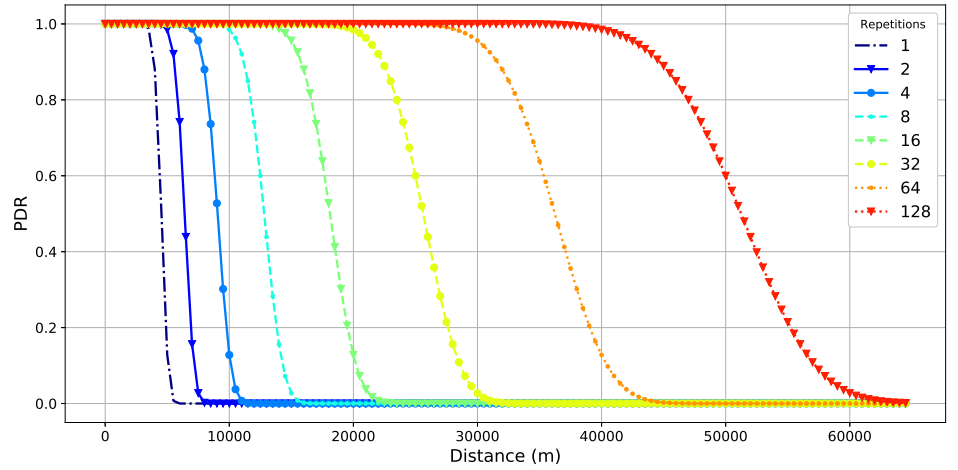

Figure 4.3: Uplink PDR as a function of distance, which was obtained using NB-DLAM by adjusting the number of repetitions. $Tones = 12$

Although similar results would be obtained for the NPDSCH channel, the coverage range would increase significantly, as the number of repetitions reaches 2048, which is 16 times greater than the NPUSCH channel. According to Equation 3.11, this would result in an equivalent increase of the resulting SNR.

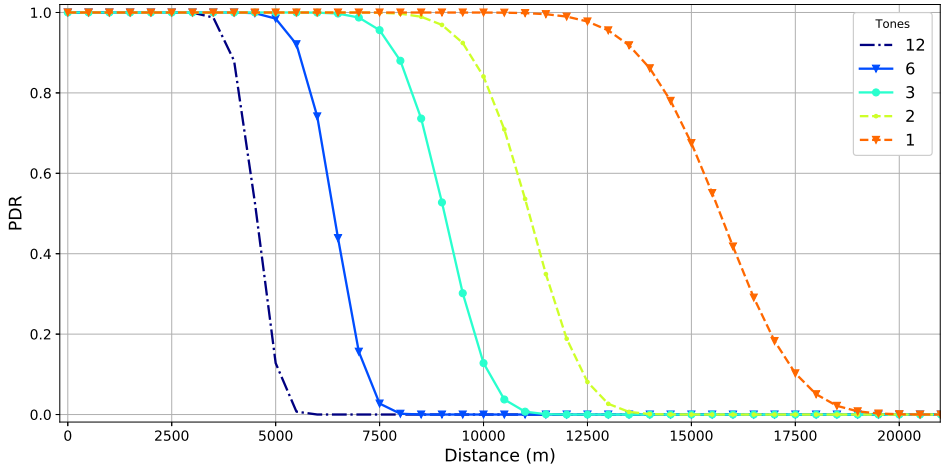

Figure 4.4: Uplink PDR as a function of distance, which was obtained using NB-DLAM by adjusting the number of tones. $Repetitions = 1$

It is evident that the number of repetitions provides a wider coverage range. The PDR_{target} can be kept up to 40000 m, adjusting the number of repetitions and 12500 m adjusting the number of tones.

Measuring the PDR values obtained with NB-DLAM, results in Figure 4.5, where it can be seen that the model can meet the PDR requirements as expected. Although, as stated before, the number of repetitions provides better coverage range when compared to the adjustment with tones. NB-DLAM discards users if the requirements can not be satisfied, hence the results presented only show values for users in good coverage range.

As explained throughout Subsection 3.3, the number of repetitions and tones have a direct impact on the achieved throughput and transmission time. This performance degradation is depicted in Figure 4.6 and Figure 4.7, respectively, obtained from Equation 3.19 and Equation 3.23.

Although, theoretically, the PDR_{target} can be kept further than depicted in Figure 4.5, the UE loses connectivity much sooner due to the other constrains. For the number of repetitions, this limitation is set by the $Throughput$, as it can be seen in Figure 4.6.

From Figure 4.6 it can be seen that adjusting the number of repetitions causes the $Throughput$ to drop bellow the minimum at 20000 m, which hinders the previously observed range of 40000 m.

In Figure 4.7, the $TransmissionTime$ values for the use of tones at around 6000 m are not represented, which means the UE was disconnected at this point. This happened due to the PDR dropping bellow the PDR_{target}, as seen in Figure 4.5.

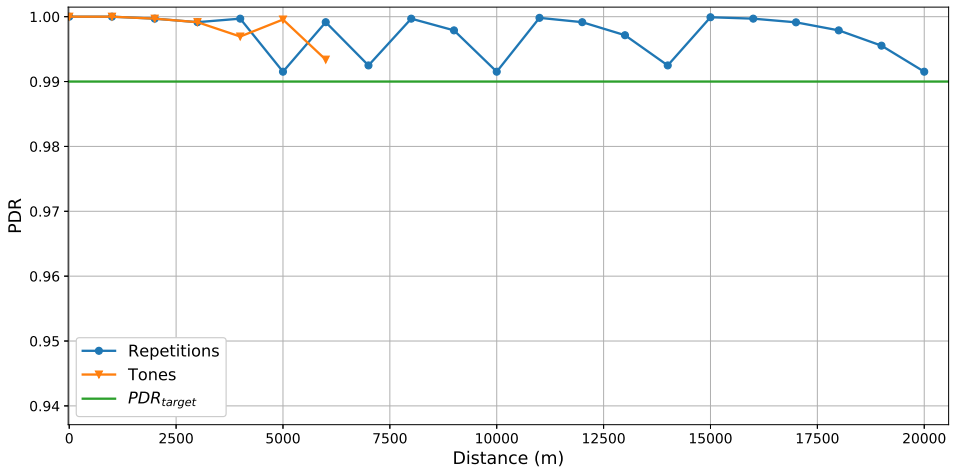

Figure 4.5: Uplink PDR, according to the NB-DLAM.

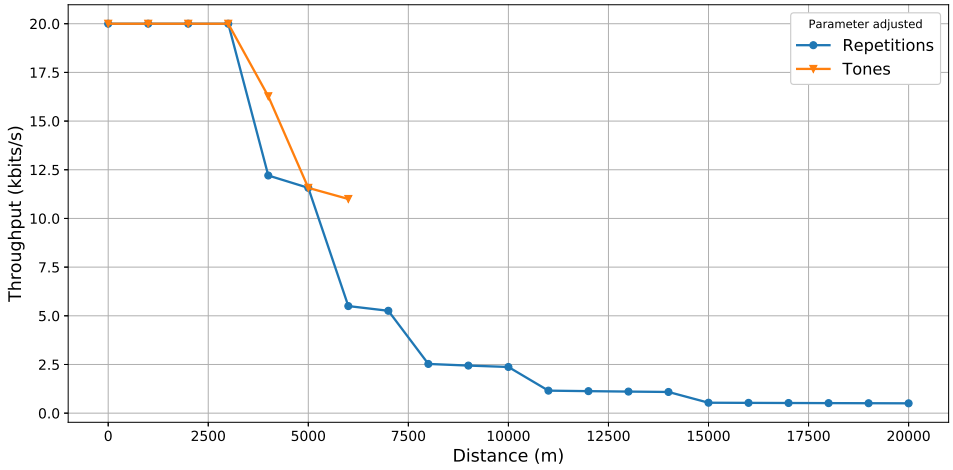

Figure 4.6: Uplink throughput achieved by NB-DLAM.

As it can be seen, the effect that the lower number of repetitions have is equivalent to the number of tones. This is explained with Equation 3.11, where the frequency factor, f, takes the same values as the available number of repetitions, N_{rep} (1, 2, 4).

4.4 NB-DLAM Validation

With the changes described in Subsection 4.2, a script in Python was developed in order to obtain, using NB-DLAM, the proper NB-IoT configurations, according to the distance between the UE and the eNB, including repetitions and tones to be used. Then it calls an ns-3 script that uses the modified ns-3 implementation, passing the repetition number and tones obtained from the model

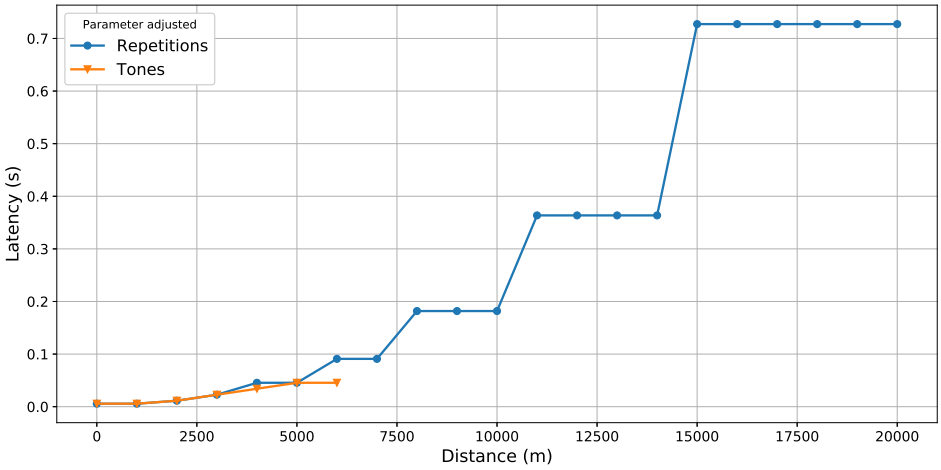

Figure 4.7: Transmission time achieved by NB-DLAM.

as command-line arguments. This interaction between the proposed model and ns-3 is depicted in Figure 4.8.

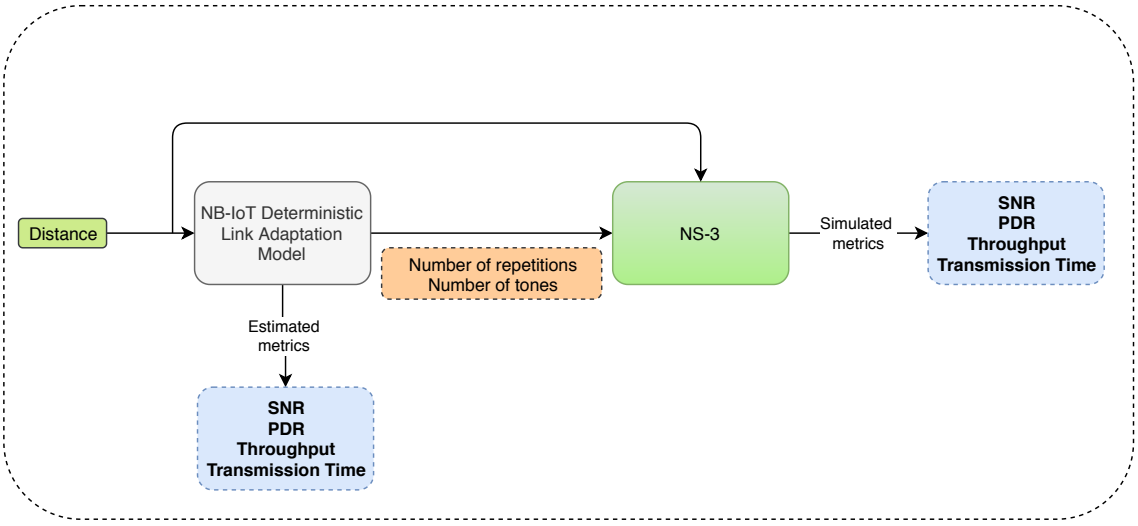

Figure 4.8: Interaction between NB-DLAM and ns-3.

For the same test scenario described in Section 4.1, an ns-3 script was used to replicate these conditions and evaluate the results estimated by the theoretical model. As ns-3 simulations are not deterministic, several simulations were run for each distance, and the results are presented with confidence intervals represented with error bars. To achieve independent results for each simulation, ns-3 provides a *SeedManager* class that can be used to provide a simulation seed and specify the run. These values can be accessed through command-line arguments (*RngSeed* and *RngRun*). All simulations share the *RngSeed* default value (1), whereas the *RngRun* is incremented at every run.

Although the conditions are the same, in ns-3, Rayleigh fading was added, not only to make it more realistic, but also because in ns-3 using only deterministic path loss propagation models, such as Log Distance, does not result in packet loss; to achieve that, it is necessary to add a stochastic propagation model to evaluate PDR. ns-3 also discards users if the QoS requirements can not be met; hence the figures showed only have values while the user is in good coverage.

As this model highly relies on the link's SNR, it is important that they are as similar as possible, as this indicates if the scenarios are the same, otherwise comparing different scenarios would not provide any valuable information. The SNR values obtained both in the model and ns-3 simulations are depicted in Figure 4.9. As expected, the SNR obtained theoretical through the model is the average of the one obtained with ns-3 (due to Rayleigh fading).

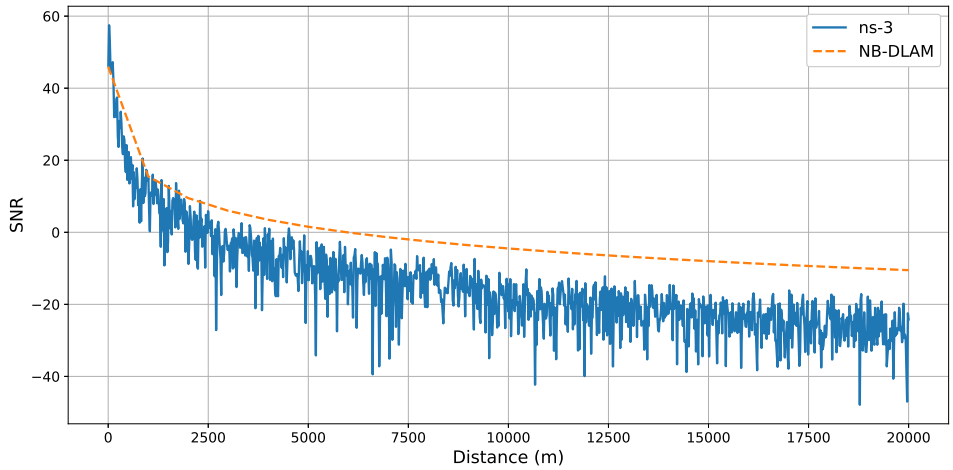

Figure 4.9: SNR: NB-DLAM vs. ns-3.

To measure the PDR in ns-3 simulation, User Datagram Protocol (UDP) Poisson traffic was generated at each position with a Poisson distribution, with a packet rate of 1000 packets/s, 2 seconds of simulation time, and 10 independent runs. After that, PDR, delay, and throughput were obtained with Equation 4.3, Equation 4.4, and Equation 4.5. Combining the previous PDR from the model, with the one obtained through the ns-3 simulations results in Figure 4.10.

NB-IoT's ability to keep a PDR at 99% for an extended range has the drawback of degrading the other QoS metrics: as latency increases significantly and throughput drops. Figure 4.11 illustrates the latency comparison between NB-DLAM and the ns-3 simulations.

NB-DLAM QoS estimations closely follow the simulation results obtained with ns-3, especially for throughput when repetitions are employed. On the other hand, when tones are used, the results obtained using NB-DLAM are not so close to the ns-3 simulation results. However, as an unstable behavior of ns-3 was experienced when tones were used, we believe that the observed difference may be justified by some ns-3 implementation bugs beyond those reported in Subsection 4.2. This paves the way for improving the implementation of ns-3, as future work.

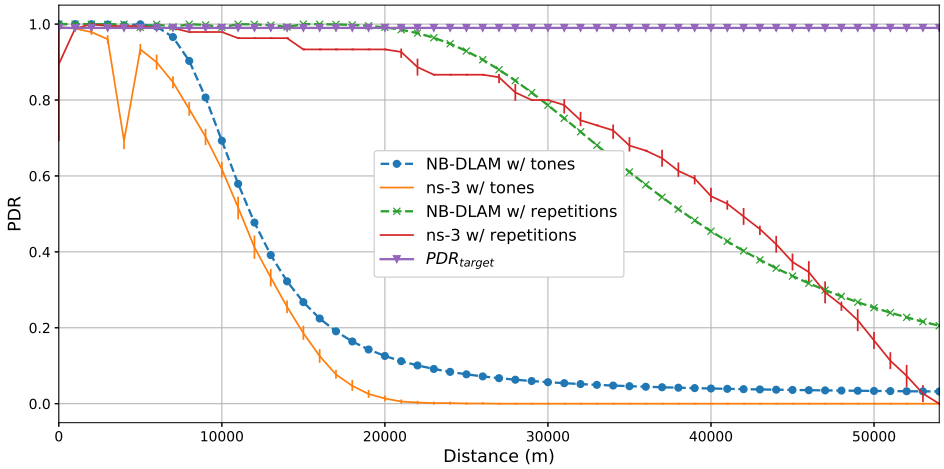

Figure 4.10: PDR: NB-DLAM vs. ns-3.

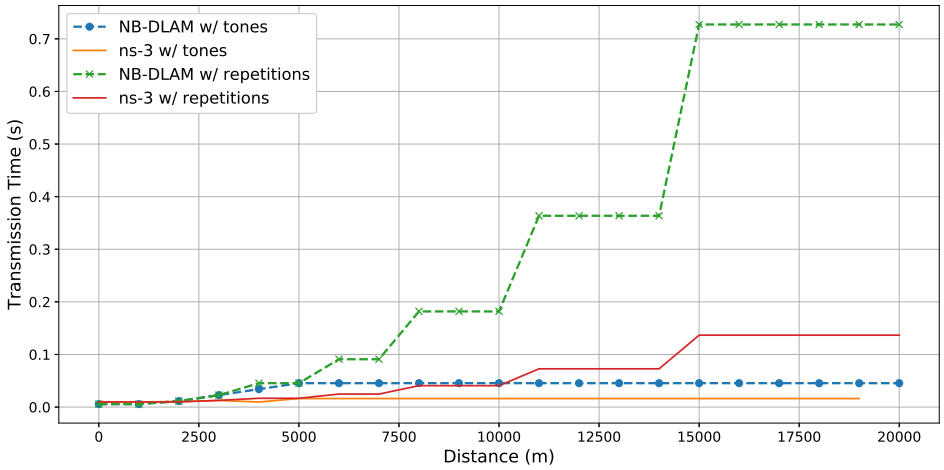

Figure 4.11: Latency: NB-DLAM vs. ns-3.

As previously observed with the NB-DLAM estimations, the use of repetitions is by far the better option, in order to achieve a higher PDR.

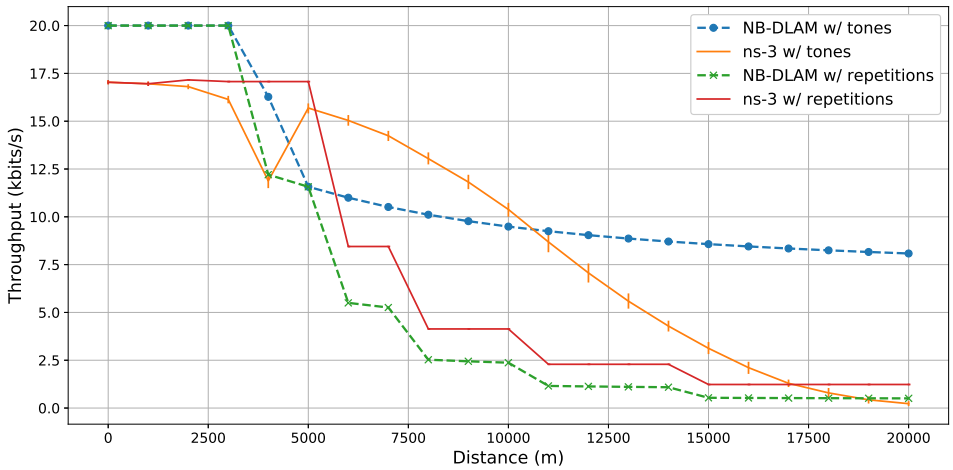

Figure 4.12: Throughput: NB-DLAM vs. ns-3.

Chapter 5

Conclusions

The exponential growth of IoT has led to an increased demand for technologies capable of answering the new requirements imposed by IoT devices, which are usually connected through IEEE 802.11. Since IEEE 802.11 is limited in range, which is a common requirement for IoT communications, cellular technologies are more suitable, as they can provide long-range communications. To answer this, 3GPP released three different technologies: EC-GSM-IoT, LTE-M, and NB-IoT. All three are expected to provide reliable communications under extreme coverage conditions, while preserving battery life and secure communications channels.

As NB-IoT can operate in a spectrum as narrow as 200 kHz, by refarming GSM carriers and reusing infrastructures, it provides an unprecedented deployment flexibility and was chosen as the study subject of this dissertation. NB-IoT provides coverage in harsh environments through the use of blind repetitions, as opposed to repetitions based on the receptor's feedback: Multi/Single tone SC-FDMA, and adaptive Modulation-Coding Scheme (MCS). Since all these configurations rely on the UE deployment conditions, this leads to the need of a network model that can predict the necessary QoS metrics and, based on those, configure the connected UEs.

This dissertation proposes a novel theoretical network planning model, NB-DLAM, that, given the distance from the UE to the serving eNB, can predict important QoS metrics, including PDR, throughput, and delay, as well as configure the UE, while complying with the strict NB-IoT requirements. NB-DLAM takes the distance between the UE and the serving eNB, calculates the path loss using the Log Distance propagation model, and estimates SNR. Based on this estimation, a theoretical BER is obtained, which enables the model to predict the communications' PDR, throughput, and delay. With these theoretical estimations, NB-DLAM calculates the optimal configurations for the number of tones and the number of repetitions, which are used to configure the UE.

To validate the accuracy of these theoretical estimations, the distance, together with the configurations obtained using NB-DLAM were imported by ns-3, and the same QoS metrics were measured and finally compared against the estimated values.

The achieved results show that the use of repetitions is better than the use of tones, since the former provides an increased coverage range, in terms of PDR (cf. Figure 4.10). While the number

of tones can keep the PDR_{target} up to 5000 m, the number of repetitions can keep this to 15000 m. Although, it is important to note that for the tones adjustment lower transmission times and higher bitrates can be achieved.

NB-DLAM estimations are similar to the simulation values obtained with ns-3, with a small error. The estimations for the PDR are the most accurate, for both repetitions and tones, which must be be denoted since PDR is the main QoS metric targeted by NB-DLAM.

5.1 Future Work

The results achieved by NB-DLAM, can be further improved in respect to the accuracy of the estimated QoS metrics, as well as additional configurations can be adjusted in order to obtain improved QoS metrics. As future work, we aim to:

- Validate the combination of the number of repetitions and the number of tones in ns-3;
- Add battery consumption estimations to NB-DLAM;
- Adjust sleep cycles to improve the battery life;
- Add coding gain and BLER theoretical estimations to NB-DLAM;
- Adjust the MCS index and the number of RU per TB (N_{ru});
- Validate NB-DLAM with all adjustable parameters combined in ns-3;
- Validate NB-DLAM by using real hardware and network emulators such as OAI;
- Validate NB-DLAM in a real networking scenario.

References

[1] 3GPP. Cellular System Support for Ultra-Low Complexity and Low Throughput Internet of Things. Technical Report (TR) 45.820, 3rd Generation Partnership Project (3GPP), 2016. URL: https://portal.3gpp.org/desktopmodules/Specifications/SpecificationDetails.aspx?specificationId=2719.

[2] Cisco Visual Networking. The Zettabyte Era: Trends and Analysis. *Cisco White Paper*, 2016.

[3] Olof Liberg, Marten Sundberg, Johan Bergman, Joachim Sachs, and Eric Wang. The Cellular Internet of Things. *Cellular Internet of Things; Academic Press: London, UK*, 2017.

[4] Min Chen, Yiming Miao, Yixue Hao, and Kai Hwang. Narrow Band Internet of Things. *IEEE Access*, 5:20557–20577, 2017. URL: http://ieeexplore.ieee.org/document/8038776/, doi:10.1109/ACCESS.2017.2751586.

[5] Jun-Bae Seo and Victor C. M. Leung. Design and Analysis of Backoff Algorithms for Random Access Channels in UMTS-LTE and IEEE 802.16 Systems. *IEEE Transactions on Vehicular Technology*, 60, 2011. URL: http://ieeexplore.ieee.org/document/6006550/, doi:10.1109/TVT.2011.2166569.

[6] F.A. Tobagi. Distributions of packet delay and interdeparture time in slotted aloha and carrier sense multiple access. *Journal of the ACM (JACM)*, 29, 1982. URL: http://dx.doi.org/10.1145/322344.322345.

[7] B. E. Benhiba, A. A. Madi, and A. Addaim. Comparative Study of the various new Cellular IoT Technologies. In *2018 International Conference on Electronics, Control, Optimization and Computer Science (ICECOCS)*, pages 1–4, 2018. doi:10.1109/ICECOCS.2018.8610508.

[8] 3GPP. Release 13, 2016. URL: http://www.3gpp.org/Release-13.

[9] CFR. e-CFR Title 47 - Telecommunication, 2019. URL: https://ECFR.io/Title-47/.

[10] ETSI. Electromagnetic compatibility and Radio spectrum Matters (ERM); Short Range Devices (SRD); Radio equipment to be used in the 25 MHz to 1000 MHz frequency range with power levels ranging up to 500 mW; Part 1: Technical characteristics and test methods. Technical report, European Telecommunications Standards Institute (ETSI), 2012. URL: https://www.etsi.org/deliver/etsi_en/300200_300299/30022001/02.04.01_40/en_30022001v020401o.pdf.

[11] ETSI. Electromagnetic compatibility and Radio spectrum Matters (ERM); Wideband transmission systems; Data transmission equipment operating in the 2,4 GHz ISM band and using wide band modulation techniques; Harmonized EN covering the essential requirements of article 3.2 of the R&TTE Directive. Technical report, European Telecommunications Standards Institute (ETSI), 2015. URL: https://www.etsi.org/deliver/etsi_en/300300_300399/300328/01.09.01_60/en_300328v010901p.pdf.

[12] Sahithya Ravi, Pouria Zand, Mohieddine El Soussi, and Majid Nabi. Evaluation, Modeling and Optimization of Coverage Enhancement Methods of NB-IoT. *arXiv:1902.09455 [cs]*, 2019. URL: http://arxiv.org/abs/1902.09455.

[13] Yassir A. Ahmad, Walid A. Hassan, and Tharek Abdul Rahman. Studying different propagation models for LTE-A system. In *2012 International Conference on Computer and Communication Engineering (ICCCE)*, Kuala Lumpur, Malaysia, 2012. IEEE. URL: http://ieeexplore.ieee.org/document/6271336/, doi:10.1109/ICCCE.2012.6271336.

[14] Andrea Goldsmith. *Wireless Communications*. Cambridge University Press, 2005.

[15] M. Hata. Empirical formula for propagation loss in land mobile radio services. *IEEE Transactions on Vehicular Technology*, 29(3), 1980. doi:10.1109/T-VT.1980.23859.

[16] Vijay Kumar Garg. *Wireless communications and networking*. The Morgan Kaufmann series in networking. Elsevier Morgan Kaufmann, Amsterdam ; Boston, 2007. OCLC: ocm76902044.

[17] Segun Popoola, Aderemi Atayero, Nasir Faruk, Carlos Calafate, Olawoyin Abiodun, and Victor Matthews. Standard propagation model tuning for path loss predictions in built-up environments. In *Computational Science and Its Applications – ICCSA 2017*, 2017. doi:10.1007/978-3-319-62407-5_26.

[18] L. M. Correia. A view of the cost 231-bertoni-ikegami model. In *2009 3rd European Conference on Antennas and Propagation*, 2009.

[19] Yuvraj Singh. Comparison of Okumura, Hata and COST-231 Models on the Basis of Path Loss and Signal Strength. *International Journal of Computer Applications*, 59(11), 2012. URL: http://research.ijcaonline.org/volume59/number11/pxc3884216.pdf, doi:10.5120/9594-4216.

[20] ITU. IoT network planning, 2016. URL: https://www.itu.int/en/ITU-D/Regional-Presence/AsiaPacific/SiteAssets/Pages/Events/2016/Dec-2016-IoT/IoTtraining/IoT%20network%20planning%20ST%2015122016.pdf.

[21] Yiming Miao, Wei Li, Daxin Tian, M. Shamim Hossain, and Mohammed F. Alhamid. Narrowband Internet of Things: Simulation and Modeling. *IEEE Internet of Things Journal*, 5(4), 2018. URL: https://ieeexplore.ieee.org/document/8010279/, doi:10.1109/JIOT.2017.2739181.

[22] S. Oh, K. Jung, M. Bae, and J. Shin. Performance analysis for the battery consumption of the 3gpp nb-iot device. In *2017 International Conference on Information and Communication Technology Convergence (ICTC)*, pages 981–983, 2017. doi:10.1109/ICTC.2017.8190831.

[23] 3GPP. Release description; Release 14. Technical report, 3rd Generation Partnership Project (3GPP), 2017. URL: http://www.3gpp.org/release-14.

[24] Andreas Hoglund, Xingqin Lin, Olof Liberg, Ali Behravan, Emre A. Yavuz, Martin Van Der Zee, Yutao Sui, Tuomas Tirronen, Antti Ratilainen, and David Eriksson. Overview of 3gpp Release 14 Enhanced NB-IoT. *IEEE Network*, 31(6), 2017. URL: http://ieeexplore.ieee.org/document/8120239/, doi:10.1109/MNET.2017.1700082.

[25] Nokia Networks. NB-IoT – Capacity evaluation. In *TDoc R1-157248*, 2015. URL: https://portal.3gpp.org/ngppapp/CreateTdoc.aspx?mode=view&contributionId=670162.

[26] Hassan Malik, Muhammad Mahtab Alam, Yannick Le Moullec, and Alar Kuusik. NarrowBand-IoT Performance Analysis for Healthcare Applications. *Procedia Computer Science*, 130:1077–1083, 2018. URL: https://linkinghub.elsevier.com/retrieve/pii/S1877050918305192, doi:10.1016/j.procs.2018.04.156.

[27] Qualcomm Inc. NB-PSS and NB-SSS Design. In *TDoc R1-161981*, 2016. URL: https://portal.3gpp.org/ngppapp/CreateTdoc.aspx?mode=view&contributionId=692517.

[28] Nitin Mangalvedhe, Rapeepat Ratasuk, and Amitava Ghosh. NB-IoT deployment study for low power wide area cellular IoT. In *2016 IEEE 27th Annual International Symposium on Personal, Indoor, and Mobile Radio Communications (PIMRC)*, Valencia, Spain, 2016. IEEE. URL: http://ieeexplore.ieee.org/document/7794567/, doi:10.1109/PIMRC.2016.7794567.

[29] Ericsson. On 5G mMTC requirement fulfilment, NB-IoT and eMTC connection density. In *TDoc R1-1703865*, 2017. URL: https://portal.3gpp.org/ngppapp/CreateTdoc.aspx?mode=view&contributionId=780666.

[30] 3GPP. Release description; Release 15. Technical report, 3rd Generation Partnership Project (3GPP), 2017. URL: https://portal.3gpp.org/desktopmodules/Specifications/SpecificationDetails.aspx?specificationId=3389.

[31] Luca Feltrin, Massimo Condoluci, Toktam Mahmoodi, Mischa Dohler, and Roberto Verdone. NB-IoT: Performance Estimation and Optimal Configuration. In *European Wireless 2018; 24th European Wireless Conference*, page 6, 2018.

[32] B. Hsieh, Y. Chao, R. Cheng, and N. Nikaein. Design of a UE-specific Uplink scheduler for NB-IoT systems. In *2018 3rd International Conference on Intelligent Green Building and Smart Grid (IGBSG)*, 2018. doi:10.1109/IGBSG.2018.8393573.

[33] Mads Lauridsen, Huan Nguyen, Benny Vejlgaard, Istvan Z. Kovacs, Preben Mogensen, and Mads Sorensen. Coverage Comparison of GPRS, NB-IoT, LoRa, and SigFox in a 7800 km^2 Area. In *2017 IEEE 85th Vehicular Technology Conference (VTC Spring)*, Sydney, NSW, 2017. IEEE. URL: http://ieeexplore.ieee.org/document/8108182/, doi:10.1109/VTCSpring.2017.8108182.

[34] Mads Lauridsen, Istvan Z. Kovacs, Preben Mogensen, Mads Sorensen, and Steffen Holst. Coverage and Capacity Analysis of LTE-M and NB-IoT in a Rural Area. In

2016 IEEE 84th Vehicular Technology Conference (VTC-Fall), Montreal, QC, Canada, 2016. IEEE. URL: http://ieeexplore.ieee.org/document/7880946/, doi:10.1109/VTCFall.2016.7880946.